This dissertation has been
microfilmed exactly as received 66-14,522

GELINAS, Robert Joseph, 1937-
FLUCTUATIONS IN RADIATION DISTRIBUTIONS.

The University of Michigan, Ph.D., 1966
Engineering, nuclear

University Microfilms, Inc., Ann Arbor, Michigan

FLUCTUATIONS IN RADIATION DISTRIBUTIONS

by
Robert Joseph Gelinas

A dissertation submitted in partial fulfillment
of the requirements for the degree of
Doctor of Philosophy in the
University of Michigan
1965

Doctoral Committee:

Professor Richard K. Osborn, Chairman
Associate Professor Ziya Akcasu
Professor William Kerr
Professor Chihiro Kikuchi
Professor George Stroke
Associate Professor George Summerfield

FLUCTUATIONS IN RADIATION DISTRIBUTIONS

by

Robert J. Gelinas

This thesis is a theoretical study of fluctuations in the radiation distributions from systems that are amenable to a transport description. We proceed by a deductive approach in which the quantum Liouville equation is used to generate a coupled set of transport equations for the first and second moments of the appropriate numbers (in fact densities) of particles that adequately describe the system. Particular attention is devoted to the description of the observables of the experiments in terms of our theoretical quantities.

The specific applications that we consider are (1) a nuclear reactor system on which we observe neutron correlation information by measurements on the high energy prompt gamma radiation field of the reactor core and (2) the Brown-Twiss correlator experiment. The latter system measures fluctuations in a mercury arc source of optical radiation by placing two photocathodes in the beam of radiation. Their outputs are fed to a correlator which measures the expectation value of the product of the fluctuations in the output currents. The observables in the reactor noise experiment are a power spectral density and the ratio of the variance to the mean of the accumulated counts from the photon detector.

In our reactor noise analysis by photon observation, we consider both a finite and an infinite reactor-detector model. It is found that the information relating to the neutron correlations of the system can in principle be observed as efficiently by photon detecting techniques as by the conventional neutron-detecting experiments. A significant advantage of a photon detecting noise experiment is that the detector can be placed outside of the reactor core proper and thereby relieve the perturbing effects that are encountered when a neutron detector is placed in-core. Also spatial effects can be effectively smoothed out because the photon detector sees a larger volume of the core than a conventional neutron detector. However it appears that photon noise measurements must still be restricted to cold, clean cores as in conventional neutron-detecting experiments. Also if one is trying to see spatially dependent effects, it is a disadvantage to use photon detection. Furthermore it is found that low power experiments are the only feasible ones (as in the conventional case).

In the Brown-Twiss experiment we find that the correlation they observed is interpretable to be due simply to geometric effects and that stimulated emission effects are apparently of no consequence in this application. In the final chapter we examine particular properties of the radiation distributions and find that even when stimulated emission is present, its effect on a fluctuation measurement

would not be seen if the energy of the radiation is much greater than that of the emitting atoms. Such "Poisson-like" sources are found to fulfill Glauber's second-order coherence condition.

ACKNOWLEDGEMENTS

My deepest expression of gratitude goes to my Committee Chairman, Professor Richard K. Osborn, for his constant and patient guidance and for the inspiring stimulation he provided at all points in this investigation. Also to Professor Ziya Akcasu go my sincere thanks for his continuing interest and for the valuable suggestions he offered in our numerous discussions relating to this work. The remaining members of my Doctoral Committee contributed generously of their time and counsel at various stages of this project, and to them also I am grateful.

In addition, I gratefully acknowledge the financial support I received from the Atomic Energy Commission (Special Fellowship in Nuclear Science and Engineering for three years) and from the Rackham School of Graduate Studies.

Inasmuch as projects of this nature can be difficult to impossible without a continuing source of strength on the "homefront," I recognize my wife, Mary, as indeed a tower of strength and devotion at every point.

TABLE OF CONTENTS

		Page
ACKNOWLEDGEMENTS		ii
LIST OF FIGURES		v
LIST OF SYMBOLS		vi
Chapter		
I.	INTRODUCTION	1
II.	GENERAL THEORY	9
III.	APPLICATION TO REACTOR NOISE ANALYSIS BY OBSERVATIONS ON HIGH ENERGY GAMMA RADIATION	20
	A. Description of the System	20
	B. Specialization of the Transport Equations	21
	1. The infinite reactor, infinite detector model	29
	2. The spatially dependent finite reactor, finite detector model	33
	C. Solutions of the Equations	37
	1. The infinite reactor and detector model	40
	a. The variance	41
	b. The power spectral density	53
	2. The finite reactor and detector model	60
	a. The power spectral density	60
	b. The variance	81
IV.	APPLICATION TO AN ANALYSIS OF THE BROWN-TWISS CORRELATOR EXPERIMENT	83
	A. Description of the System	83
	B. Specialization of the Transport Equations	84
	C. The Experimental Observables	88
	D. A Qualitative Interpretation of the Results of Brown and Twiss	91

V. GENERAL PROPERTIES OF RADIATION DISTRIBUTIONS 99

A. Specialization of the Equations for Photon Singlet and Doublet Densities 100
B. Solutions of the Equations and Discussion 102

REFERENCES 108

LIST OF FIGURES

Figure		Page
1	Ratio of Variance to Mean Minus One versus Gate Width for Photon Detecting Noise Experiment	48
2	The Power Spectral Density versus Frequency for Photon Detecting Noise Experiment	56
3	Diagram of Finite Reactor, Finite Detector System	70
4	A Schematic Diagram of the System for the Brown and Twiss Correlator Experiment	85
5	A Schematic Diagram to Exhibit the Role of the Half-Silvered Mirror in the Brown-Twiss Correlator Experiment	93
6	Ideal Correlation Factor versus Detector Separation in Brown-Twiss Correlator Experiment	96

LIST OF SYMBOLS

In order to achieve greater continuity in the presentation of the main text, some of the more frequently used symbols are defined here. We will list the equation in which a given symbol first appears whenever possible. In the event that the same symbol is used for different quantities, the appropriate meaning will be clear from the context.

$A(D_1 \cap D_2)$ — Relative overlap of detectors 1 and 2, Eqn (153)

$B_\alpha^J(\underline{k}'', \underline{k})\, d^3k$ — The probability that a fission induced by a neutron with wave vector $\underline{k}''$ will produce J prompt neutrons of which α will have $\underline{k} \in d^3k$, Eqn (17)

$B_{\alpha\beta}^J(\underline{k}''|\underline{k}', \underline{k})\, d^3k'\, d^3k$ — The probability that a fission induced by a neutron with wave vector $\underline{k}''$ will produce J prompt neutrons of which α will have $\underline{k}' \in d^3k'$ and β will have $\underline{k} \in d^3k$. When $\underline{k} = \underline{k}'$, $B_{\alpha\beta}^J(\underline{k}''|\underline{k}', \underline{k}) \to \delta_{\alpha\beta}\, \delta(\underline{k} - \underline{k}')\, B_\alpha^J(\underline{k}'', \underline{k})$, Eqn (19)

$(C.R.)_\gamma$ — Count rate due to gamma detection, Eqn (94)

$(C.R.)_N$ — Count rate due to neutron detection, Eqn (92)

C — Speed of light, Eqn (13)

$D(t)$ — Density operator for system, Eqn (1)

E_o	—	Threshold energy of detection process
$\mathcal{P}^D(\underline{x}' \to \underline{\kappa})\, d^3\kappa$	—	The probability that a photon with wave vector $\underline{x}'$ will, upon detection by a photoelectric detector, produce a photoelectron with wave vector $\underline{\kappa} \in d^3\kappa$, Eqn (11)
$\mathcal{P}^{Sc}(\underline{k}'' \to \underline{k})\, d^3k$	—	The probability that a neutron with initial wave vector $\underline{k}''$ will be scattered into a final wave vector $\underline{k} \in d^3k$, Eqn (17)
$F_1^A(\underline{X}, \underline{\kappa}, a, t)$	—	Coarse grained density of Ath type particle or photon, with quantum label "a." Eqn (1)
$F_2^{AB}(\underline{X}, \underline{\kappa}, a; \underline{X}', \underline{\kappa}', b; t)$	—	Coarse grained doublet or cross density for "A" and "B" type particles and/or photons with quantum state labels "a" and "b" respectively, Eqn (2)
$f_1^A(\underline{X}, \underline{\kappa}, t)$	—	Singlet density for "particles" of kind "A", Eqn (12)
$f_2^{AB}(\underline{X}, \underline{\kappa}, \underline{X}', \underline{\kappa}', t)$	—	Doublet or cross densities for "particles" of kinds "A" and/or "B," Eqn (11)
$(f_1^N)_S$	—	neutron singlet density averaged over the volume V_S , Eqn (146)
$G^{(11)}(\underline{X}, \underline{X}, t)$	—	Glauber's first order correlation function, Eqn (211)
$G^{(22)}(\underline{X}, \underline{X}', \underline{X}', \underline{X}; t)$	—	Glauber's second order correlation function, Eqn (212)

$G_\eta^Q(\underline{k}'', \underline{x})d^3x$ — The probability that a fission event induced by a neutron at $\underline{k}''$ will produce exactly Q photons, η of which have $\underline{x} \in d^3x$, Eqn (13)

$G_{\eta\nu}^Q(\underline{k}''|\underline{x}, \underline{x}')d^3x\, d^3x'$ — The probability that a fission event induced by a neutron at $\underline{k}''$ will produce Q photons, η of which have $\underline{x} \in d^3x$ and ν of which have $\underline{x}' \in d^3x'$. When $\underline{x} = \underline{x}'$ $G_{\eta\nu}^Q(\underline{k}''|\underline{x}, \underline{x}') \to \delta_{\eta\nu}\delta(\underline{x}-\underline{x}')G_\eta^\nu(\underline{k}'', \underline{x})$, Eqn (15)

H — Hamiltonian for system, Eqn (3)

$H(t)$ — Unit step function, Eqn (11)

$\mathcal{A}$ — Disadvantage factor, Eqn (155)

$\mathcal{J}(t)$ — Detector current, Eqn (56)

$\langle J \rangle$ — Expected number of prompt neutrons born per fission event

$\underline{K}$ — Wave vector associated with momentum $\hbar\underline{K}$

L — Dimension of cell in configuration space

M — Mean value of detected particles, Eqn (77)

m_β — Mass of photoelectron, Eqn (11)

$(N_i^N)_R$ — Total number of neutrons in the reactor, Eqn (159)

$(N_i^N)_s$ — Number of neutrons in the volume V_s, Eqn (158)

$\mathcal{Q}$ — The ideal correlation factor in the Brown-Twiss correlator experiment, Eqn (181)

$\mathcal{P}$ — Reactor power (watts), Eqn (86)

$\mathcal{R}_{AB}(\underline{\kappa} \rightarrow \underline{\kappa}')$ — Probability per unit $\underline{\kappa}$ -volume that a "particle" of type "A" with wave vector $\underline{\kappa}$ is absorbed and a "B"-type "particle" is subsequently re-emitted, Eqn (10) with $\underline{\kappa}'$.

r — Interaction rate, Eqn (11)

$S(\underline{x},\underline{k})\,d^3x\,d^3k$ — The expected number of neutrons produced per second in d^3x about $\underline{x}$, and in d^3k about $\underline{k}$, by means other than the fission process, Eqn (16).

S_0 — Source strength of photons from mercury arc, Eqn (178)

S_ν — Number of photons born per unit volume per sec., Eqn (145)

s — Variable of Laplace transformation, Eqn (62)

$T_a(a,\underline{\kappa}\,|\,\underline{\kappa}_1,a_1;\underline{\kappa}_2,a_2)$ — Transition probability per atom for the absorption of an "A" type particle with wave vector $\underline{\kappa}$ and quantum state label "a." The initial and final states of the source atoms are designated by $\underline{\kappa}_1, a_1$ and $\underline{\kappa}_2, a_2$ respectively, Eqn (8)

$T_e(a,\underline{\kappa}\,|\,\underline{\kappa}_1,a_1;\underline{\kappa}_2,a_2)$ — Transition probability per atom for the emission of an "A" type "particle," Eqn (8)

$T_{n'n}$ — Transition probability per unit time, Eqn (6)

T_R — Resolving time of the correlator in the Brown and Twiss experiment, Eqn (181)

$U(\underline{k})$ or $U(\nu)$ — Radiation energy density, Eqn (208)

V — Contributions to the energy of the system exclusive of the particle kinetic energies, Eqn (4)

$V_a = V_R = R.V.$ — Volume of reactor, Eqns (85), (138a), and (156)

$V_D = D.V.$ — Volume of detector, Eqns (61) and (84)

V_{Si} — Volume seen by i^{th} detector, Eqn (144)

$V(t)$ — Variance of detected particles, Eqn (73)

$\underline{v}^A$ — Velocity of "A^{th}" type particle or photon, Eqn (6)

$\underline{X}$ — Position vector locating the center of a spatial cell

Greek Characters

α — Specific power, Eqn (86)

$\alpha(\underline{k})$ — Photon absorption rate, Eqn (197)

$\alpha(\underline{X})$ — Annihilation operator, Eqn (211)

$\alpha^{\dagger}(\underline{X})$	—	Creation operator, Eqn (211)
$\mathcal{E}_{k}$	—	Photon energy, Eqn (204)
$\epsilon(\underline{k})$	—	Photon emission rate, Eqn (197)
$\Gamma(\underline{X}, \underline{k}) d^3X d^3k$	—	The expected number of photons produced per second in d^3X about $\underline{X}$ and in d^3k about $\underline{k}$ by extraneous photon sources, Eqn (13)
λ	—	Photon polarization index
λ_a	—	Absorption mean free path for photons, Eqn (133)
$\langle \mu \rangle$	—	First angular moment of the neutron scattering frequency, Eqn (121)
$\langle \eta \rangle$	—	Expectation value of the effective number of prompt photons born per fission event, Eqn (27)
$\langle \eta'^2 \rangle$	—	Expected square of the effective number of prompt photons born per fission event, Eqn (29)
$\underline{\Omega}$	—	Direction of travel for particle or photon
$\Omega_1(z, a)$	—	Solid angle efficiency factor, Eqn (151)
ω	—	Frequency of power spectrum
ν_{λ}	—	Frequency of radiation with polarization λ

$\Phi(\omega)$	—	Power spectral density, Eqn (58)
$\varphi(\tau)$	—	Autocorrelation function, Eqn (56)
$\Phi^{\gamma}(\underline{X})$	—	Flux of photons arriving at $\underline{X}$, Eqn (144)
$\rho^{A}(\underline{X}, \underline{K}, a)$	—	Number operator of A^{th} type particle or photon with quantum label "a," Eqn (1)
Σ	—	Macroscopic cross section
θ	—	Energy of emitting atoms of the photon source, Eqn (204)
$\psi_n(\underline{X})$	—	Reactor modes, Eqn (138b)

I. INTRODUCTION

In this dissertation we analyze the statistical fluctuations in the radiation distributions of two specific systems. The first system is that of a nuclear reactor in which the radiation of interest is emitted characteristically by neutron-nuclear interactions. The second system is one in which the radiation is emitted by a mercury arc discharge. The observations on the latter system, which we will soon discuss in greater detail, may be well known to some as the Brown-Twiss experiment.

The approaches taken for interpreting fluctuation phenomena are diverse in scope and most often phenomenological in nature. We will not attempt to survey the literature on this point, but will give adequate references for the particular applications which are of concern subsequently. Of course in real (many-body) systems upon which experiments are performed one is generally attempting to infer information about microscopic causal mechanisms from observations on macroscopic quantities. The main contribution of the present work is to explore from the start, in a deductive manner, the connection between experimentally observable quantities and their "driving mechanisms."

The observation of fluctuations of a given quantity, say a density of charged particles, about its mean value is a convenient context within which to work, and we shall do so. The concept of

fluctuations calls for the introduction of a joint probability density that relates to the microscopic system. By a joint probability density, we mean one which describes the probability for all "particles" of the system to be jointly distributed in phase space in a given manner as a function of time. The term "particles" here is extended to refer to photons as well as to ordinary particles. The deductive approach that we employ departs from phenomenological approaches at the point where phenomenological treatments arrive at an equation for the joint probability density by various plausibility arguments. The deductive approach recognizes that this probability density satisfies the Liouville equation , and further deductions are drawn therefrom. Thus we proceed from rather basic statistical axioms to deduce the appropriate balance equations for relevant particle and photon densities that describe the system of interest to the order that the observations are carried out.

In particular in the quantum formalism, which we will employ for reasons given below, the mean density (singlet density) of a given type of "particle" is expressed theoretically as the expectation value of the appropriate number operator for the density of that type of "particle." This is a first order stochastic quantity and is just the first moment of the probability density with the number operator. In order to consider fluctuations about the mean, it is necessary to consider second order stochastic quantities which we will refer to as doublet densities. These are expectation values of second order

monomials of the appropriate number operators. A measure of the fluctuations of a given distribution of particles or photons can then be obtained through a variance. The variance is defined as the difference between the doublet density of interest and the product of the corresponding singlet densities.

The work presented in this dissertation considers applications to systems that fulfill conditions that render them amendable to transport theoretic analysis. The term "transport theory" is used in the generic sense here, in that we are concerned with equations that describe the averages of first and second order monomials of number operators in phase space (higher orders are not considered because the observations on the systems we consider are sufficiently described by first and second order averages). Such a treatment is readily adaptable to interpreting energy transfer fluctuation measurements, and we shall concern ourselves exclusively with this class of systems. That is, we are considering applications which clearly involve the transfer of energy in rather discrete quanta from one type of "particle" distribution to another. "Particles" are simply thought of here as well-localized concentrations of mass, or of charge, or of energy, etc.

The transport theoretic approach or particulate point of view may be contrasted to the "field theoretic"approach. The field theory (or wave theory) is couched in terms of averages of odd-order monomials of creation and destruction operators. Terms that are first order in creation or destruction operators are usually referred to as

field operators. In fact many physical measurements are indeed sensitive to expectation values of field operators. A case in point is the large class of experiments in electrodynamics which are sensitive to expectation values of electric and/or magnetic field operators, which are in turn described by Maxwell's equations. Another case where field theory is useful is in neutron diffraction experiments. In this case the observable is interpreted in terms of the expectation value of the neutron field operator, $\langle \psi \rangle$. A field equation for $\langle \psi \rangle$ can be derived analogously to Maxwell's equations for electromagnetic fields. What we are then saying is that the question of whether an experiment is to be interpreted in terms of a transport theoretic formalism or by a wave theoretic formalism is necessarily dictated by the nature of the actual observation that is to be made on the real system, and whether that observation is sensitive primarily to discrete energy transfer phenomena or to wave phenomena. One can now recognize a very broad "middle class" of experiments where both wave and particulate phenomena are at play. These can be anticipated, perhaps, to be the most troublesome experiments to interpret theoretically. The applications which are considered in the present work are felt to be very definitely of the type that should yield to a transport theoretic analysis, and we shall attempt to strengthen this point as the analysis is developed in each case.

The organization of the material in this dissertation is as follows. The general theory involving the deduction of the appropriate

sets of transport equations for the analysis of fluctuations in radiation distributions is presented in Chapter II. The first application, considered in Chapter III, analyzes fluctuations in the distributions of gamma radiation from a nuclear reactor in order to obtain neutron correlation information about the reactor system. In Chapter IV the second application is devoted to an analysis of the Brown-Twiss correlator experiment. This experiment observes the fluctuations in the photon distributions from a mercury arc optical source.

With regard to Chapter III it can be noted that studies of fluctuations and correlations in neutron distributions are conventionally approached from the point of view that an experimental investigation will be based upon the direct detection of neutrons.* Our work suggests that in principle it is possible to perform reactor noise experiments by detecting the high energy prompt fission gamma radiation ($E_o \geq 5$ Mev) generated by neutron interactions within the core. Gammas emitted by (n , γ) interactions will be seen to behave as prompt gammas accompanying fission events. Detection of prompt gammas is possible in the type of experiments to be discussed, namely those in which the ratio of the variance to mean and the power spectral density are measured for the charged particles arising from photon detections, because it is suggested that only delayed gamma radiation emitted in the time interval between 10^{-4} seconds and 1 second

*An exception is an experiment performed at Pennsylvania State University in which an attempt was made to observe neutron fluctuations by monitoring the Cerenkov radiation. (1)

after a fission event affects the interpretation of the measurement adversely. However, it is inferred from the work of Maienschein, et al[2] that there is negligible delayed gamma emission due to fission-product decay in this time interval. Delayed gamma emission in shorter time intervals (less than 10^{-4} seconds after fission) behaves as prompt and it is also a negligible fraction of the total gamma energy emitted per fission event. Long-lived fission products will be troublesome in the sense that they are the source of considerable background due to low energy pile-up.

However, Chapman et al[3] show that for the Bulk Shielding Reactor II the delayed gamma radiation with energies greater than 5 Mev is considerably less than that arising promptly (within 10^{-4} seconds) from fission and (n , γ) interactions. Thus by suitable photon energy discrimination techniques and adequate shielding (to reduce low energy pile-up) it appears that the necessary information may be obtained in practice for neutron noise analysis by photon detection. This type experiment will most likely be limited to clean reactors for the present as in conventional neutron detecting noise experiments. If suitable threshold detectors can be found, however, this requirement could be removed to great advantage.

With these introductory remarks in mind on practical aspects of the problem, the theoretical development will indicate the striking similarity of neutron correlations by photon detection with the better-known theory of conventional neutron correlation studies. An infinite

reactor, infinite detector model and a finite reactor-detector model will be examined.

In Chapter IV we apply transport theory to the analysis of the Brown-Twiss correlator experiment.[4] In this experiment a beam of light from a mercury arc source is filtered (4358 A) and imaged upon a pinhole .019 cm in diameter. The beam from the secondary source is split with a half-silvered mirror, and the resulting beams are detected with photocathodes located so that the optical paths from the source are equal for each detector. The outputs of the detectors are then fed to a correlator which observes the expectation value of the product of the fluctuations in the detector output currents as a function of the relative positions of the two detectors. The absence of modal and diffraction effects in this system suggest the relevance of the transport theoretic approach that we employ. The transport theory also enjoys the facility of convenient applicability to inhomogeneous systems such as this one. The interpretation of the Brown-Twiss effect that we obtain from this point of view, based upon our theoretical description of the actual observables of their system, are in good qualitative agreement with the experimental results they obtained. We then propose an experiment that would interpret this effect from a direct measurement of the ratio of the variance to the mean of the detected particle accumulations as a function of the detector positions in the same basic system as above. This measurement is attractive because the

cumulants of the detected particles are the deduced quantities of the theory and can be measured directly in principle as well.

In Chapter V we consider particular properties of the radiation distributions. The characteristics of "Poisson-like" and non-"Poisson-like" radiation distributions are examined, and the relevance of these characteristics to measurements on given systems is discussed. Finally we indicate some connections between Glauber's field formalism (specifically the "coherence conditions" he formulates in terms of his "correlation functions") and the results we have obtained by a transport theoretic treatment.

II. GENERAL THEORY

Since a connection between the theory of fluctuations and their measurement is conveniently established through the variance of the detected particles or through the power spectral density of their detection rates, this investigation proceeds from the appropriate coupled set of singlet and doublet equations descriptive of the system. The deduction of this set of transport equations can be accomplished in various ways. One of the more familiar phenomenological approaches was performed by Matthes.[5] Others[6][7] employ the principles of stochastic analysis. Still other viewpoints are adopted to this end in the field of optics. The work of Glauber[8] has extensive references to the latter. As was pointed out in the Introduction, we employ a quantum mechanical treatment in which number densities are defined as expectation values of appropriate operators, and the equations for these densities are derived from the quantum Liouville equation. There are at least three reasons for using a quantum approach.

In the first place the quantum formalism is naturally adaptable to systems in which particles or photons are created or destroyed. Both of the applications we consider are prime examples of such systems. Secondly, one is faced with the questionable interpretation of an ordinary density in phase space. That is, $f(\underline{x}, \underline{p}, t)\, d^3x\, d^3p$ is ordinarily taken to represent the expected number of particles, say, to be found in the phase volume $d^3x\, d^3p$ about $(\underline{X}, \underline{p})$ at time t.

However in the limiting sense of small $d^3x\, d^3p$ the interpretation breaks down, at least with regard to particle distributions, due to the uncertainty principle; and if this density is not interpretable in the limiting sense, then how? The quantum theory averts this difficulty by defining an appropriate number operator to represent the number of particles (and photons) in a given phase cell of sufficient volume. Finally it is expected that quantum mechanical distributions of particles or photons should be implicit in the structure of the transport equations. In the case of thermalized neutrons, for instance, the neutron balance equations are expected to yield a Fermi-Dirac velocity distribution as opposed to a Maxwellian. Of course the measurements we consider on a reactor system will undoubtedly be insensitive to this distinction. However in the case of photon distributions one might expect quantum effects to have somewhat greater significance,and these should therefore be examined.

It can be seen further that the applications considered in this work are rather convenient special cases within the broad scope of the many-body problem. First of all, both the reactor system and the Brown-Twiss system that we consider are examples of systems in which energy is transferred and in which modal and diffraction effects are absent for all intents and purposes. Thus transport theory is indicated at the outset. Furthermore, it can be recognized that in these particular radiation systems it is a good approximation to ignore the interactions of photons with other photons. Thus the

mathematical description of photon distributions is linear up to the point where the photons influence the particle distributions in the system. It has been pointed out previously[9] that neutron distributions in reactors are similarly one of the simplest many-body systems. In addition to the fact that neutron-neutron interactions can be neglected, such systems as a nuclear reactor also allow the binary collision approximation. This is because neutron-nuclear forces are extremely short range. Therefore with these general remarks in mind and in light of our introductory remarks, we delve directly into the deduction of the transport equations that will apply to the above-mentioned systems.

The techniques employed in this procedure have been presented in sufficient detail previously in applications to reactor systems[10], neutral gases[11], and plasmas[12][13]. Thus an attempt will be made here to present the essence of the principles involved, and the calculational detail will be abbreviated in light of the references that deal with these details. So let us proceed by dividing the six dimensional phase space into hypercells of volume $(2\pi)^3$ where configuration space is divided into non-overlapping cells of volume L^3 and $\underline{K}$-space into cells of volume $\frac{(2\pi)^3}{L^3}$. Here $\underline{K}$ is the wave vector associated with a momentum $\hbar\,\underline{K}$. The center of a hypercell is located by coordinates $(\underline{X}, \underline{K})$, and all "particles" (recall that we include photons in this set as well as ordinary particles) in the cell are located by giving these co-ordinates.

The singlet densities for particles of kind "A" are defined by

$$F_1^A(\underline{X},\underline{K},a,t) \equiv \frac{1}{(2\pi)^3}\, Tr\, \rho^A(\underline{X},\underline{K},a)\, D(t) \tag{1}$$

and the doublet densities for particles of kinds "A" and "B" by

$$F_2^{AB}(\underline{X},\underline{K},a;\underline{X}',\underline{K}',b;t) \equiv \frac{1}{(2\pi)^6}\, Tr\, \rho^A(\underline{X},\underline{K},a)\,\rho^B(\underline{X}',\underline{K}',b)\, D(t)\,. \tag{2}$$

The operators $\rho^A(\underline{X},\underline{K},a)$ are number operators whose eigenvalues in a diagonalizing representation represent the possible numbers of particles of kind "A" in the phase-space hypercell centered at the point $(\underline{X},\underline{K})$. The labels "a" (and "b") specify the quantum numbers necessary to complete the description of the particle's state. They designate such things as polarization, spins, and internal states. All particles in a given phase cell are assigned the coordinates of the center of the cell, their momenta being given by $\underline{P} = \hbar\,\underline{K}$. The volume of the cells is $(2\pi)^3$. Evidently these phase points are discretely distributed; however, whenever appropriate, they will be assumed to be sufficiently dense to be regarded as a continuum. The quantity D is the density operator for the system. The system is comprised of all of the particles of all kinds necessary for a model adequate to the interpretation of a given experiment.

The density operator is assumed to satisfy the Liouville equation given by

$$\frac{\partial D(t)}{\partial t} = \frac{i}{\hbar}[D, H] \quad , \tag{3}$$

where H is the Hamiltonian of the system. It is useful to write H as

$$H = \sum_A H^A + V \quad . \tag{4}$$

In this case H^A describes the kinetic energy of the "A"-type particle (this includes the contribution from the free photon field), and V represents all other contributions to the energy of the system.

The first step in the present derivation of a transport equation is to display (generically)

$$\frac{F(t+\tau) - F(t)}{\tau} = \frac{\partial F}{\partial t}\left[1 + \frac{\tau}{2}\,\frac{\partial^2 F/\partial t^2}{\partial F/\partial t} + \cdots\right]$$

$$\simeq \frac{\partial F}{\partial t} \quad , \tag{5}$$

for sufficiently small τ and for densities which do not vary too rapidly in time. For example, if $F(t) \sim e^{t/T}$, then the above approximation implies the neglect of a series of terms, the largest of

which is $\mathcal{O}(\tau/T)$ for $\frac{\tau}{T} < 1$. An obvious lower limit for τ is interaction times; which, in the case that we will consider, will not likely exceed 10^{-10} seconds. It is to be noted that this approximation (coarse-graining in time) is a necessity and not merely a calculational trick, since it is meaningless to compare densities at two instants closer together than an interaction time.

It can then be shown[9][10] that, in a representation which diagonalizes the number operator, the equation for the singlet density of the "A"-type particles can be written as

$$\left[\frac{\partial}{\partial t} + \underline{v}^{A}\cdot\underline{\nabla}\right] F_1^{A}(\underline{x},\underline{k},a;t) = \frac{1}{(2\pi)^3}\sum_{n n'}\left[\rho^{A}_{n'n'}(\underline{x},\underline{k},a) - \rho^{A}_{nn}(\underline{x},\underline{k},a)\right] (*)$$

$$(*)\; T_{n'n}\, D_{nn}(t) \quad +$$

$$+ \text{terms off-diagonal in } D(t) \,. \qquad (6)$$

We have introduced $\underline{v}^{A}$ to represent the velocity of the "A"-type particles. Note that $\underline{v}^{A} \equiv \hbar\underline{k}/m_A$ when "A" applies to an ordinary particle, and m_A is the mass of the particle. When "A" applies to photons, $\underline{v}^{A} \equiv c\,\underline{\Omega}$ and $c = 3 \times 10^{10}$ cm/sec because the medium is non dispersive for the radiation of interest. The direction vector for the photons is given by $\underline{\Omega}$. $T_{n'n}$ stands for the probability per unit time for a transition to occur between an initial state designated by n and a final state designated by n'. The summation over

n and n' includes all initial and final states. Expressions for $T_{n'n}$ can be obtained by conventional perturbation techniques. Many approximations are required to go from equations (1), (3), and (5) to equation (6). All of these approximations have been displayed elsewhere explicitly, some interpreted qualitatively, but few estimated quantitatively. Since many of these considerations have been dealt with specifically in references (9), (10), and (13), which are directed more toward the actual development of a transport theory, we proceed at this point to writing the generic doublet equation (neglecting terms proportional to off-diagonal elements of $D(t)$ henceforth) as:

$$\left[\frac{\partial}{\partial t} + \underline{v}^{A}\cdot\underline{\nabla} + \underline{v}^{B}\cdot\underline{\nabla}'\right] F_2^{AB}(\underline{x},\underline{\kappa},a;\underline{x}',\underline{\kappa}',b;t) = \frac{1}{(2\pi)^3}\sum_{nn'} T_{n'n}(x)$$

$$(x)\left[\rho^{A}_{n'n'}(\underline{x},\underline{\kappa},a)\rho^{B}_{n'n'}(\underline{x}',\underline{\kappa}',b) - \rho^{A}_{nn}(\underline{x},\underline{\kappa},a)\rho^{B}_{nn}(\underline{x}',\underline{\kappa}',b)\right] D_{nn}(t). \qquad (7)$$

Note that the gradients which appear in the equations at this point are symbolic and have the meaning of a finite difference in the density of interest at two adjacent cells in configuration space, divided by the linear dimension of the cells. They will take on the usual meaning of gradients when we pass to the continuum for densely spaced points.

Further specialization of these equations requires considering individually the relevant interactions on the right hand side of the

balance equations. To do this it is useful to restrict our attention to the dependence of the transition probability, $T_{n'n}$, upon occupation numbers only. Typically $T_{n'n}$ is proportional to ρ_{nn} for processes in which a particle is destroyed. When a particle is created, $T_{n'n}$ is proportional to $[1 \pm \rho_{nn}]$, where the plus and minus signs go with bosons and fermions respectively. If, in the creation of a particle, ρ_{nn} is not negligible compared to unity, the effect of quantum statistics will be observed.

Incorporating these remarks into the computation which further reduces the right hand side of equations (6) and (7), we get

$$\left[\frac{\partial}{\partial t} + \underline{v}^{A} \cdot \underline{\nabla}\right] F_1^{A}(\underline{X}, \underline{K}, t) = \frac{1}{(2\pi)^3} \sum_{n,a} D_{nn}(t) \left\{ \left[1 \pm \rho_{nn}^{A}(\underline{X}, \underline{K}, a)\right] (x) \right.$$

$$(x) \sum_{\substack{A', \underline{K}_1, a_1 \\ \underline{K}_2, a_2}} \rho_{nn}^{A'}(\underline{X}, \underline{K}_1, a_1)\, T_e(a, \underline{K} | \underline{K}_1, a_1; \underline{K}_2, a_2) -$$

$$\left. - \rho_{nn}^{A}(\underline{X}, \underline{K}, a) \sum_{\substack{A', \underline{K}_1, a_1 \\ \underline{K}_2, a_2}} \rho_{nn}^{A'}(\underline{X}, \underline{K}_1, a_1)\, T_a(a, \underline{K} | \underline{K}_1, a_1; \underline{K}_2, a_2) \right\} . \tag{8}$$

Note that

$$F_1^{A}(\underline{X}, \underline{K}, t) = \sum_{a} F_1^{A}(\underline{X}, \underline{K}, a; t) \tag{9a}$$

and

$$\rho^{A}(\underline{X},\underline{K}) = \sum_{a} \rho^{A}(\underline{X},\underline{K},a) \quad . \tag{9b}$$

The quantity $T_e(a,\underline{K}|\underline{K}_1,a_1;\underline{K}_2,a_2)$ is the transition probability per atom for the emission of an "A"-type particle with wave vector $\underline{K}$ and quantum state label "a." The state of the atom prior to undergoing a transition is designated by $\underline{K}_1, a_1$. The wave vector associated with the atom in its initial state is $\underline{K}_1$, and a_1 represents the initial internal state of the atom. Then $\underline{K}_2$, a_2 are defined analogously for final states of the atom (after a transition). The quantity $T_a(a,\underline{K}|\underline{K}_1,a_1;\underline{K}_2,a_2)$ represents the transition probability per atom for the absorption of an "A"-type particle with wave vector $\underline{K}$ and quantum labels, a. The initial and final states of the atom involved in the transition are designated by $\underline{K}_1, a_1$ and $\underline{K}_2, a_2$ respectively as above. It can be noted that the transition probabilities for absorption and emission processes are symmetric under the interchange of the initial and final states. Since we are considering emission and/or absorption of single particles, only those final states for which $\left[\rho^{A}_{n'n'}(\underline{X},\underline{K},a) - \rho^{A}_{nn}(\underline{X},\underline{K},a)\right]$ is plus or minus one, respectively, are contributors from the summation over all states. In like manner as in (8) we can write the set of doublet equations (once again restricting A and B to photons and

particles relevant to our description of a given system) as:

$$\left[\frac{\partial}{\partial t} + \underline{v}^{A}\cdot\underline{\nabla} + \underline{v}^{B}\cdot\underline{\nabla}'\right] F_2^{AB}(\underline{X},\underline{K};\underline{X}',\underline{K}';t) = \frac{1}{(2\pi)^6} (\times)$$

$$(\times)\sum_{n,a,b} D_{nn}(t)\Big\{\left[1 \pm \rho_{nn}^{A}(\underline{X},\underline{K},a)\right]\rho_{nn}^{B}(\underline{X}',\underline{K}',b)\sum_{\substack{A',\underline{K}_1,a_1\\ \underline{K}_2,a_2}}\rho_{nn}^{A'}(\underline{X},\underline{K}_1,a_1)(\times)$$

$$(\times)\, T_e(a,\underline{K}\,|\,\underline{K}_1,a_1\,;\,\underline{K}_2,a_2) + \left[1 \pm \rho_{nn}^{B}(\underline{X}',\underline{K}',b)\right](\times)$$

$$(\times)\,\rho_{nn}^{A}(\underline{X},\underline{K},a)\sum_{\substack{B',\underline{K}_1,b_1\\ \underline{K}_2,b_2}}\rho_{nn}^{B'}(\underline{X}',\underline{K}_1,b_1)\,T_e(b,\underline{K}'\,|\,\underline{K}_1,b_1\,;\,\underline{K}_2,b_2) -$$

$$-\rho_{nn}^{A}(\underline{X},\underline{K},a)\,\rho_{nn}^{B}(\underline{X}',\underline{K}',b)\Big[\sum_{\substack{A',\underline{K}_1,a_1\\ \underline{K}_2,a_2}}\rho_{nn}^{A'}(\underline{X},\underline{K}_1,a_1)(\times)$$

$$(\times)\, T_a(a,\underline{K}\,|\,\underline{K}_1,a_1\,;\,\underline{K}_2,a_2) + \sum_{\substack{B',\underline{K}_1,b_1\\ \underline{K}_2,b_2}}\rho_{nn}^{B'}(\underline{X}',\underline{K}_1,b_1)(\times)$$

$$(\times)\, T_a(b,\underline{K}'\,|\,\underline{K}_1,b_1\,;\,\underline{K}_2,b_2)\Big] + (2\pi)^3\,\delta(\underline{X}-\underline{X}')\,\delta(\underline{K}-\underline{K}')(\times)$$

$$(\times)\,\delta_{AB}\Big[\left(1 \pm \rho_{nn}^{A}(\underline{X},\underline{K},a)\right)\sum_{\substack{A',\underline{K}_1,a_1\\ \underline{K}_2,a_2}}\rho_{nn}^{A'}(\underline{X},\underline{K}_1,a_1)(\times)$$

$$(\times) T_e(a,\underline{K}|\underline{K}_1,a_1;\underline{K}_2,a_2) + \rho^{A}_{nn}(\underline{X},\underline{K},a)\sum_{\substack{A',\underline{K}_1,a_1\\ \underline{K}_2,a_2}} \rho^{A'}_{nn}(\underline{X},\underline{K}_1,a_1)(\times)$$

$$(\times)\, T_a(a,\underline{K}|\underline{K}_1,a_1;\underline{K}_2,a_2)\Big] - (2\pi)^3\,\delta(\underline{X}-\underline{X}')\,(1-\delta_{AB})\,(\times)$$

$$(\times)\rho^{A}_{nn}(\underline{X},\underline{K},a)\,\mathcal{R}_{AB}(\underline{K}\to\underline{K}')\Big\}\,. \qquad (10)$$

The quantity $\mathcal{R}_{AB}(\underline{K}\to\underline{K}')d^3K'$ is simply the probability per unit $\underline{K}$ -volume that a particle of type "A" with wave vector $\underline{K}$ is absorbed and a "B"-type particle is subsequently re-emitted with wave vector $\underline{K}'\epsilon d^3K'$.

Further reduction of the transport equations from their present form requires the consideration of the more specific characteristics of a particular system; Chapters III and IV, which are specifically devoted to applications, give such specializations.

III. APPLICATION TO REACTOR NOISE ANALYSIS BY OBSERVATIONS ON HIGH ENERGY GAMMA RADIATION

A. Description of the System

The model we employ for the reactor system that is observed by the detection of photons may be described in the following manner. Only photons with energies greater than E_o are observed. We have seen that a judicious energy threshold for observing prompt photons from a reactor is $E_o \geq 5$ Mev, because only a small tail of the distribution of delayed gammas occurs above 5 Mev in comparison with the number of prompt gammas in this energy range. It is also reasonable to assume that only a very small fraction of the photons in this high-energy range have previously undergone a scattering interaction and maintained a final energy greater than 5 Mev[3]. Also bremsstrahlung (mean energy of .5 Mev) is a negligible photon source for $E_o \geq 5$ Mev. For the sake of discussion it is assumed that a scintillator is used to detect photons, and the photoelectrons that result from the scintillations interacting with the photocathode material are simply recorded and accumulate in time. Photo fission is neglected, and photons are assumed not to interact with other photons. The only photon interactions that are considered to be relevant in this model are those events by which a photon appears to be absorbed. Detection processes, photoelectric absorption, and pair production are the obvious photon absorbing interactions. Photon

scattering is also taken to behave as a means of absorption here, because we assumed that a photon is removed from the energy range of interest by a scattering interaction. The emission of photons and particles by neutron interactions is taken to be isotropic, and extraneous neutron and photon sources are assumed to be isotropic and constant in time. Finally we neglect delayed neutrons and delayed photons for expediency of calculation.

B. Specialization of the Transport Equations

In this system we are interested only in charged particles from detection events, neutrons, and photons. All other distributions in the system are assumed to be known. To deduce the interaction terms on the right hand side of the balance equations, it is well to restrict our attention to the dominant interactions that affect the system. In the present case the dominant processes are neutron fission, capture, and scattering; the production of gamma radiation by fission and (n , γ) events; the absorption of gammas by the medium; and the detection process. Neutrons scattered by neutrons are neglected.

In the types of systems with which we are dealing, it has been found[10][12] that about all the information that is necessary regarding $T_{n'n}$ is its dependence upon occupation numbers in the types of interactions we are considering. For example, when particles or photons are destroyed, $T_{n'n}$ is proportional to the occupation number of the particle or photon that is destroyed. In creation

processes $T_{n'n}$ is characteristically proportional to $[1 \pm \rho]$, where the plus sign applies to bosons and the minus sign to fermions. In the present application ρ is neglected in comparison to unity in the case of creation processes, because the measurements on these systems will be insensitive to effects peculiar to quantum statistics. This may or may not be allowable in other applications such as the Brown-Twiss experiment to be discussed in Chapter IV.

The final reduction of equations (9) and (10) is carried out in the same manner as employed previously in the literature[10][13]. Upon performing that task and passing to the continuum, where one assumes that the discrete points in phase space are sufficiently closely spaced that they can be treated as continuous, we can finally write the set of working equations for this system as:

$$\left[\frac{\partial}{\partial t} + \frac{\hbar}{m_\beta}\left(\underline{K}\cdot\underline{\nabla} + \underline{K}'\cdot\underline{\nabla}'\right)\right] f_2^{\beta\beta'}(\underline{X},\underline{K};\underline{X}',\underline{K}';t) = \int d^3K''(x)$$

$$(x)\, r_D(K'')\Big[\mathcal{J}^D(\underline{K}''\to\underline{K})\, f_2^{\lambda\beta'}(\underline{X},\underline{K}'';\underline{X}',\underline{K}';t) + \mathcal{J}^O(\underline{K}''\to\underline{K}')(x)$$

$$(x)\, f_2^{\beta\lambda'}(\underline{X},\underline{K};\underline{X}',\underline{K}'';t)\Big] H(t) + \delta(\underline{X}-\underline{X}')\,\delta(\underline{K}-\underline{K}')(x)$$

$$(x)\int d^3K''\, r_D(K'')\,\mathcal{J}^D(\underline{K}''\to\underline{K})\, f_1^{\lambda}(\underline{X},\underline{K}'';t)\, H(t) \quad .$$

$$\left[\frac{\partial}{\partial t} + \frac{\hbar}{m_\beta}\underline{K}\cdot\underline{\nabla}\right] f_1^{\beta}(\underline{X},\underline{K},t) = \int d^3K'' \nu_0(K'')\, \mathcal{P}^0(\underline{K}''\to\underline{K})\, f_1^{\lambda}(\underline{X},\underline{K}'',t)\, H(t)$$

(12)

$$\left[\frac{\partial}{\partial t} + c\,\underline{\Omega}'\cdot\underline{\nabla}' + \frac{\hbar}{m_\beta}\underline{K}\cdot\underline{\nabla} + \nu_a(K')\right] f_2^{\beta\lambda'}(\underline{X},\underline{K};\underline{X}',\underline{K}';t) =$$

$$= \int d^3K''\, \nu_0(K'')\, \mathcal{P}^0(\underline{K}''\to\underline{K})\, f_2^{\lambda\lambda'}(\underline{X},\underline{K}'';\underline{X}',\underline{K}';t)\, H(t) +$$

$$+ \int d^3k''\, \nu_f(k'')\, f_2^{\beta N'}(\underline{X},\underline{K};\underline{X}',\underline{k}'';t) \sum_{Q,\eta} \eta\, G_\eta^Q(\underline{k}'',\underline{K}') +$$

$$+ f_1^{\beta}(\underline{X},\underline{K},t)\,\Gamma(\underline{X}',\underline{K}') - \delta(\underline{X}-\underline{X}')\,\nu_D(K')\,\mathcal{P}^0(\underline{K}'\to\underline{K})\,(*)$$

$$(*)\; f_1^{\lambda}(\underline{X},\underline{K}',t)\, H(t)$$

(13)

and $f_2^{\lambda\beta'}(\underline{X},\underline{K};\underline{X}',\underline{K}';t)$ is obtained by interchanging arguments.

$$\left[\frac{\partial}{\partial t} + c\,\underline{\Omega}\cdot\underline{\nabla} + r_a(k)\right] f_1^{\lambda}(\underline{x},\underline{k},t) = \int d^3k''\, r_f(k'')\, f_1^{N}(\underline{x},\underline{k}'',t)(x)$$

$$(x)\sum_{Q,\eta}\eta\, G_\eta^Q(\underline{k}'',\underline{k}) + \Gamma(\underline{x},\underline{k})\,.$$

(14)

$$\left[\frac{\partial}{\partial t} + c(\underline{\Omega}\cdot\underline{\nabla} + \underline{\Omega}'\cdot\underline{\nabla}') + r_a(k) + r_a(k')\right] f_2^{\lambda\lambda'}(\underline{x},\underline{k};\underline{x}',\underline{k}';t) =$$

$$= f_1^{\lambda}(\underline{x},\underline{k},t)\,\Gamma(\underline{x}',\underline{k}') + \Gamma(\underline{x},\underline{k})\, f_1^{\lambda'}(\underline{x}',\underline{k}',t) + \int d^3k''\, r_f(k'')(x)$$

$$(x)\sum_{Q,\eta}\eta\left\{G_\eta^Q(\underline{k}'',\underline{k})\, f_2^{N\lambda'}(\underline{x},\underline{k}'';\underline{x}',\underline{k}';t) + G_\eta^Q(\underline{k}'',\underline{k}')(x)\right.$$

$$\left.(x)\, f_2^{\lambda N'}(\underline{x},\underline{k};\underline{x}',\underline{k}'';t)\right\} + \delta(\underline{x}-\underline{x}')\int d^3k''\, r_f(k'')\, f_1^{N}(\underline{x},\underline{k}'',t)(x)$$

$$(x)\sum_{Q,\eta,\nu}\eta\nu\, G_{\eta\nu}^Q(\underline{k}''\,|\,\underline{k},\underline{k}') + \delta(\underline{x}-\underline{x}')\,\delta(\underline{k}-\underline{k}')\,(x)$$

$$(x)\left[r_a(k)\, f_1^{\lambda}(\underline{x},\underline{k},t) + \Gamma(\underline{x},\underline{k})\right]$$

(15)

$$\left[\frac{\partial}{\partial t} + \frac{\hbar}{m_N}\underline{k}\cdot\underline{\nabla} + L(\underline{k})\right] f_1^N(\underline{X},\underline{k},t) = S(\underline{X},\underline{k}) \ ,$$

(16)

where

$$L(\underline{k}) f_1^N(\underline{X},\underline{k},t) = r_t(k) f_1^N(\underline{X},\underline{k},t) - \int d^3k''\left[r_s(k'')(x)\right.$$

$$\left. f^{Sc}(\underline{k}''\to\underline{k}) + r_f(k'')\sum_{J,\alpha}\alpha B_\alpha^J(\underline{k}'',\underline{k})\right] f_1^N(\underline{X},\underline{k}'',t) \ .$$

(17)

$$\left[\frac{\partial}{\partial t} + \frac{\hbar}{m_N}(\underline{k}\cdot\underline{\nabla} + \underline{k}'\cdot\underline{\nabla}') + L(\underline{k}) + L(\underline{k}')\right] f_2^{NN'}(\underline{X},\underline{k};\underline{X}',\underline{k}';t) =$$

$$= f_1^N(\underline{X},\underline{k},t) S(\underline{X}',\underline{k}') + S(\underline{X},\underline{k}) f_1^{N'}(\underline{X}',\underline{k}',t) + \delta(\underline{X}-\underline{X}')(x)$$

$$(x)\,\delta(\underline{k}-\underline{k}') S(\underline{X},\underline{k}) + \delta(\underline{X}-\underline{X}')\Lambda(\underline{X};\underline{k},\underline{k}';t) \ ,$$

(18)

where

$$\Lambda(\underline{X};\underline{k},\underline{k}';t) = \delta(\underline{k}-\underline{k}')\Big\{ r_t(k) f_1^N(\underline{X},\underline{k},t) + \int d^3k''\; r_s(k'')_{(x)} \mathcal{J}^{sc}(\underline{k}''\to\underline{k})\, f_1^N(\underline{X},\underline{k}'',t)\Big\} - \Big[r_s(k)\,\mathcal{J}^{sc}(\underline{k}\to\underline{k}') + r_f(k)_{(x)} \sum_{J,\alpha}{}_{(x)}\,\alpha\, B_\alpha^J(\underline{k},\underline{k}')\Big] f_1^N(\underline{X},\underline{k},t) - \Big[r_s(k')\,\mathcal{J}^{sc}(\underline{k}'\to\underline{k}) + r_f(k')_{(x)} \sum_{J,\alpha}{}_{(x)}\,\alpha\, B_\alpha^J(\underline{k}',\underline{k})\Big] f_1^{N'}(\underline{X}',\underline{k}',t) + \int d^3k''\; r_f(k'') \sum_{J,\alpha,\beta}{}_{(x)}\,\alpha\beta\; B_{\alpha\beta}^J(\underline{k}''\,|\,\underline{k},\underline{k}')\, f_1^N(\underline{X},\underline{k}'',t)$$

(19)

$$\Big[\frac{\partial}{\partial t} + \hbar\Big(\frac{\underline{K}\cdot\underline{\nabla}}{m_p} + \frac{\underline{k}'\cdot\underline{\nabla}'}{m_n}\Big) + L(\underline{k}')\Big] f_2^{\beta N'}(\underline{X},\underline{K};\underline{X}',\underline{k}';t) = \int d^3K''\; r_D(K'')\,\mathcal{J}^D(\underline{K}''\to\underline{K})\, f_2^{\lambda N'}(\underline{X},\underline{K}'';\underline{X}',\underline{k}';t)\,H(t) + f_1^\beta(\underline{X},\underline{K},t)\,S(\underline{X}',\underline{k}')\,,$$

(20)

and $f_2^{N\beta'}(\underline{X},\underline{k};\underline{X}',\underline{K}';t)$ is obtained by interchanging arguments.

$$\left[\frac{\partial}{\partial t} + c\underline{\Omega}\cdot\underline{\nabla} + \frac{\hbar}{m_N}\underline{k}'\cdot\underline{\nabla}' + r_a(k) + L(\underline{k}')\right] f_2^{\lambda N'}(\underline{X},\underline{k};\underline{X}',\underline{k}';t) =$$

$$= \Gamma(\underline{X},\underline{k}) f_1^{N'}(\underline{X}',\underline{k}',t) + f_1^{\lambda}(\underline{X},\underline{k},t)\, S(\underline{X}',\underline{k}') + \int d^3k''\, r_f(k'')^{(x)}$$

$$^{(x)} f_2^{NN'}(\underline{X},\underline{k}'';\underline{X}',\underline{k}';t) \sum_{Q,\eta} \eta\, G_\eta^Q(\underline{k}'',\underline{X}) - \delta(\underline{X}-\underline{X}')\, r_f(k')^{(x)}$$

$$^{(x)} f_1^N(\underline{X},\underline{k}',t) \sum_{Q,\eta} \eta\, G_\eta^Q(\underline{k}',\underline{X}) \quad , \qquad (21)$$

and $f_2^{N\lambda'}(\underline{X},\underline{k};\underline{X}',\underline{k}';t)$ is obtained by interchanging arguments. (Note that many of the terms in these equations were defined in the List of Symbols, so that greater continuity could be attained in the presentation of the text at this point.)

To this point the multiplet densities are general for all real times. However, experiments will be interpreted in terms of accumulations of charged particles in view of the fact that a physical measurement is to run positively in time starting from, say, t = 0 to time t. Thus the step function $H(t)$ is employed above in expressions describing the detection of photons. It is seen that the charged particle multiplet densities are continuous functions in time and

represent accumulations of charged particles. The rates of accumulation, i.e., the first time derivatives of charged particle multiplets are discontinuous, having been zero at times prior to t = 0 and non zero for $t \geq 0$ due to the observation starting at t = 0. It is then noted that the second time derivatives of charged particle multiplets are singular at t = 0. Thus we have seen that the consequences of this restricted validity are conveniently accounted for by interpreting the counting rate per photon, r_D, as proportional to the step function, $H(t)$, which has the properties:

$$H(t) = 0 \qquad t < 0 \tag{22}$$

$$H(t) = 1 \qquad t \geq 0, \tag{23}$$

and

$$\frac{dH(t)}{dt} = \delta(t) . \tag{24}$$

The following list defines the quantities appearing in the above equations that were heretofore undefined:

(a) The superscripts on the densities designate the type of "particle" referred to as:

N ⟶ neutrons

β ⟶ photoelectrons (are the detected particles)

λ ⟶ photons

(b) $\Sigma_s(k)$ is the probability per unit path for small paths that a neutron with momentum of magnitude $\hbar k$ will be scattered. The interaction rates expressed by r's are

just the product of the macroscopic cross sections and the mean speeds of the relevant particles. The subscripts for interactions of interest are:

S ——► neutron scattering

f ——► fission

a_N ——► neutron absorption

t ——► total neutron events

c ——► capture of neutrons

a ——► photon absorption

D ——► detection of photons by photoelectric material

1. The infinite reactor, infinite detector model

Having the equations of the previous section, it is desired at this point to reduce them to a form which is readily amenable to solution and is yet convenient for subsequent interpretation. The reduction of the set of transport equations is gross in some respects and is performed in many instances without a great deal of experimental or theoretical justification. However, others[10] have shown that a gross treatment is at least a reasonable first step in order to gain a clear insight into the fundamental phenomena involved but yet does not suggest that the omitted detail is, in the long run, negligible. So we obtain the set of equations appropriate to the infinite reactor and infinite detector model by integrating the equations over all space and directions and noting that there is no streaming. The photon detector is assumed to be uniformly distributed over the entire reactor. Thus

$\Sigma_a(\mathcal{E})$ is composed of $\Sigma_D(\mathcal{E})$ plus the cross sections for all other types of photon absorption. Neutron densities are integrated over all energies, and both the neutron and photon densities are assumed to be stationary. As indicated previously in the description of the system, we wish to count only those photoelectrons that correspond to photons with energies greater than 5 Mev. Therefore the relevant equations will be integrated over the appropriate ranges of photoelectron and photon energies. All system parameters such as reaction rates r_3, r_f, r_{aN}, r_t, r_c, r_a, r_D, and the mean neutron speed $\langle v_N \rangle$ have now become energy averaged quantities. When working with singlet equations, singlet densities are the weight functions for this averaging procedure. Likewise doublet densities are the weight functions when these averages are taken in doublet equations. We then assume that the energy-averaged system parameters are independent of the density that is used as the weight function.

Performing this sequence of computations, the set of equations becomes

$$\frac{\partial f_1^{\beta}(t)}{\partial t} = r_D f_1^{\lambda} H(t) \tag{25}$$

$$\frac{\partial f_2^{\beta\beta}(t)}{\partial t} = \left[2 r_D f_2^{\beta\lambda}(t) + r_D f_1^{\lambda} \right] H(t) \tag{26}$$

$$\left[\frac{\partial}{\partial t} + r_a\right] f_2^{\beta\lambda}(t) = r_D\left[f_2^{\lambda\lambda} - f_1^{\lambda}\right] H(t) + \langle\eta\rangle r_f f_2^{\beta N}(t) + f_1^{\beta}(t)\,\Gamma \tag{27}$$

$$\left[\frac{\partial}{\partial t} + a_1\right] f_2^{\beta N}(t) = r_D f_2^{\lambda N} H(t) + f_1^{\beta}(t)\,S \tag{28}$$

$$f_2^{\lambda\lambda} = \frac{\langle\eta\rangle r_f}{r_a} f_2^{N\lambda} + \frac{\langle\eta'^2\rangle r_f}{2 r_a} f_1^{N} + \frac{f_1^{\lambda}}{2} + \frac{\Gamma}{r_a}\left[f_1^{\lambda} + \frac{1}{2}\right] \tag{29}$$

$$f_2^{N\lambda} = \frac{1}{r_a + a_1}\left[\langle\eta\rangle r_f\left(f_2^{NN} - f_1^{N}\right) + S f_1^{\lambda} + f_1^{N}\Gamma\right] \tag{30}$$

$$f_1^{\lambda} = \frac{\langle\eta\rangle r_f}{r_a} f_1^{N} + \frac{\Gamma}{r_a} \tag{31}$$

$$f_1^{N} = \frac{S}{a_1} \tag{32}$$

$$f_2^{NN} = \left[f_1^{N}\right]^2 + \frac{c_1 + a_1}{2 a_1} f_1^{N} \quad , \tag{33}$$

where we have used, in general, for the "Ath" type of particle or

photon

$$r f_1^{\wedge}(t) = \int d^3\underline{x} \int d^3\kappa \; f_1^{\wedge}(\underline{x}, \underline{\kappa}, t)\, r(\kappa) \quad . \tag{34}$$

The following notation has been introduced with the reduction:

(a) $\langle J \rangle$ is the expected number of prompt neutrons produced per fission.

(b) $\langle \eta \rangle$ is defined as the expected effective number of prompt gammas per fission event. That is if we let $\langle \eta \rangle_f$ be the expected number of prompt photons born per fission event in the absence of (n, γ) interactions, $\langle \eta \rangle$ can be written as

$$\langle \eta \rangle = \frac{\langle \eta \rangle_f r_f + \langle \eta \rangle_{n\gamma} r_{n\gamma}}{r_f} \quad , \tag{35}$$

where

$\langle \eta \rangle_{n\gamma} \equiv$ expected number of prompt photons born per (n, γ) event. That this is permissible can be seen in the course of deducing the equations where $r_{n\gamma} \langle \eta \rangle_{n\gamma}$ is recognized to be structurally analogous to $r_f \langle \eta \rangle_f$.

(c) $\langle \eta'^2 \rangle$ is defined as the expected square of the effective number of prompt photons born per fission event.

(d) $$a_1 \equiv \nu_{aN} - \langle J \rangle \nu_f = \nu_{aN}(1-k) \tag{36}$$

(e) $$c_1 \equiv \nu_c + \langle (J-1)^2 \rangle \nu_f \ . \tag{37}$$

In addition to the present oversimplified infinite model, we will also consider a more realistic system in which the spatially dependent, finite features of the system will be retained. So before finally going to the actual deduction of solutions for the equations we have at present, let us first carry out the appropriate reduction for the spatially dependent, finite reactor and detector model.

2. The spatially dependent, finite reactor and detector model

In this system the photon detectors are assumed to be scintillators placed at points $\underline{X}$ and $\underline{X}'$ outside the core. The equations are integrated over photoelectron energies and over relevant photon energies. Once again a threshold detector is used to detect photons with $E_o = \hbar c \kappa_o \geq 5$ Mev. Streaming of photoelectrons is neglected, and consistent P-1 approximation procedures are applied to the set of all neutron densities and cross densities. Neutron quantities are again integrated over all neutron energies, and energy averaged system parameters are taken to be independent of the density that is used as the weight function. The emission of photons and neutrons by neutron events has been assumed throughout to be isotropic. Likewise the emission of neutrons by external sources is taken to be isotropic, uniform, and constant in time.

Photon and neutron densities and neutron currents are assumed to be stationary, and the extraneous gamma source, Γ , is neglected for expediency.

Performing this reduction, the set of equations becomes

$$\frac{\partial f_1^{\beta}(\underline{x},t)}{\partial t} = \Delta f_1^{\lambda}(\underline{x})\, H(t) \tag{38}$$

$$\frac{\partial f_2^{\beta\beta'}(\underline{x},\underline{x}',t)}{\partial t} = \left\{\Delta f_2^{\lambda\beta'}(\underline{x},\underline{x}'t) + \Delta' f_2^{\beta\lambda'}(\underline{x},\underline{x}',t)\right\} H(t) +$$

$$+ \delta(\underline{x}-\underline{x}')\,\Delta f_1^{\lambda}(\underline{x})\, H(t) \tag{39}$$

$$\left[\frac{\partial}{\partial t} + B_{\gamma'}\right] f_2^{\beta\lambda'}(\underline{x};\underline{x}',\underline{\Omega}';t) = \Delta f_2^{\lambda\lambda'}(\underline{x};\underline{x}',\underline{\Omega}')\, H(t) +$$

$$+ \frac{P_\gamma}{4\pi} f_2^{\beta N'}(\underline{x},\underline{x}',t) - \delta(\underline{x}-\underline{x}')\, r_D f_1^{\lambda}(\underline{x},\underline{\Omega}')\, H(t) \tag{40}$$

$$B_\gamma f_1^{\lambda}(\underline{x},\underline{\Omega}) = \frac{P_\gamma}{4\pi} f_1^{N}(\underline{x}) \tag{41}$$

$$\left[B_\gamma + B_{\gamma'}\right] f_2^{\lambda\lambda'}(\underline{x}, \underline{\Omega}; \underline{x}', \underline{\Omega}') = \frac{P_\gamma}{4\pi}\left\{f_2^{N\lambda'}(\underline{x}; \underline{x}', \underline{\Omega}') + f_2^{\lambda N'}(\underline{x}, \underline{\Omega}; \underline{x}')\right\} +$$

$$+ \delta(\underline{x} - \underline{x}')\left\{\frac{P_{\gamma\gamma'}}{(4\pi)^2} f_1^N(\underline{x}) + \delta(\underline{\Omega} - \underline{\Omega}') r_a f_1^\lambda(\underline{x}, \underline{\Omega})\right\} . \tag{42}$$

The following new notation has been introduced:

$$\Delta f^\lambda(\underline{x}) \equiv \int d^3k \; r_D(k) f^\lambda(\underline{x}, \underline{k}) . \tag{43}$$

The subscript has intentionally been deleted, because this notation applies for all photon densities and cross densities.

Also

$$\Delta' f^{\lambda'}(\underline{x}') \equiv \int d^3k' \; r_D(k') f^{\lambda'}(\underline{x}', \underline{k}') \tag{44}$$

$$B_\gamma \equiv c\,\underline{\Omega}\cdot\underline{\nabla} + r_a \tag{45}$$

$$B_{\gamma'} \equiv c\,\underline{\Omega}'\cdot\underline{\nabla}' + r_a . \tag{46}$$

$$\frac{P_\gamma}{4\pi} f^N(\underline{X}) = P_\gamma(\underline{\Omega}) f^N(\underline{X}) \equiv \int d^3k''\, r_f(k'') \langle \eta(\underline{\Omega}) \rangle f^N(\underline{X}, \underline{k}'')$$

$$= \frac{\langle \eta \rangle r_f}{4\pi} f^N(\underline{X}) \qquad (47)$$

where

$\langle \eta(\underline{\Omega}) \rangle \equiv$ expected number of photons that are born into $d\Omega$ about $\underline{\Omega}$ by a fission event. (48)

$$\frac{P_{\gamma\gamma'}}{(4\pi)^2} f^N(\underline{X}) = P_{\gamma\gamma'}(\underline{\Omega}, \underline{\Omega}') f^N(\underline{X}) \equiv \int d^3k''\, r_f(k'') \langle \eta(\underline{\Omega}) \nu(\underline{\Omega}') \rangle^{(\times)}$$

$$(\times) f^N(\underline{X}, \underline{k}'')$$

$$= \frac{\langle \eta \nu \rangle}{(4\pi)^2} r_f f^N(\underline{X}) \qquad (49)$$

where

$\langle \eta(\underline{\Omega}) \nu(\underline{\Omega}') \rangle d\Omega d\Omega' \equiv$ expected product of the number of photons, η, born into $d\Omega$ about $\underline{\Omega}$ jointly with ν born into $d\Omega'$ about $\underline{\Omega}'$ by a fission event. (50)

It has been shown by Akcasu[14] that the class of distributions to which $\langle \eta(\Omega)\, \nu(\Omega') \rangle$ belongs has the property:

$$\int d\Omega \int d\Omega' \langle \eta(\Omega)\, \nu(\Omega') \rangle = \langle \eta'^{2} \rangle \,. \tag{51}$$

C. Solutions of the Equations

Before solving the sets of reduced equations, we should briefly examine the observable quantities in the experiments that are commonly used for noise analysis. The noise experiments we will consider are those which measure the ratio of the variance to mean of the charged particles and those which measure the power spectral density.

The variance to mean experiment is conveniently performed by recording the output pulses of the individual detection events by some suitable means, such as on a recording tape. The variance is computed by dividing the recorded data into equal time intervals of width τ. Then by squaring the number of counts in each interval, summing these results, and dividing by the number of intervals, one gets the mean square value of the counts accumulated in τ. But this is just $f_2^{\beta\beta}(\tau)$. By varying τ, we get the detected particle doublet as a function of τ. The mean value is obtained by summing the number of counts in the intervals of width τ and dividing by the number of intervals. This is $f_1^{\beta}(\tau)$. The variance is

$f_2^{\beta\beta}(\tau) - [f_1^{\beta}(\tau)]^2$. As was indicated previously, $f_1^{\beta}(\tau)$ and $f_2^{\beta\beta}(\tau)$ represent accumulations over the interval τ because of the initial conditions that were applied to all β densities.

These initial conditions are:

$$f_1^{\beta}(0) = 0 \tag{52}$$

$$f_2^{\beta\beta}(0) = 0 \tag{53}$$

$$f_2^{\beta\lambda}(0) = f_2^{\lambda\beta}(0) = 0 \tag{54}$$

$$f_2^{\beta N}(0) = f_2^{N\beta}(0) = 0 \quad . \tag{55}$$

The definition employed here for the power spectral density, $\Phi(\omega)$, is the cosine transform of the autocorrelation function $\varphi(\tau)$. The autocorrelation function relevant to the measurements with which we are concerned is the autocorrelation function of the output current, $\mathcal{J}(t)$, from the photon detector. The computation of $\Phi(\omega)$ can be performed analytically by processing the raw data from an FM tape, for instance, which might be used to record the output current from the detector; or suitable electronic equipment utilizing a succession of filters among other circuitry can be used to give $\Phi(\omega)$ directly from the output current. The autocorrelation function is given for stationary currents by:

$$\varphi(\tau) = \langle \mathcal{J}(t)\, \mathcal{J}(t+\tau) \rangle \quad . \tag{56}$$

It can be shown[15] that

$$\varphi(\tau) = \frac{1}{2} \frac{\partial^2 f_2^{\beta\beta}(\tau)}{\partial \tau^2} \tag{57}$$

which then gives the power spectral density as:

$$\Phi(\omega) = \frac{1}{2} \int_{-\infty}^{\infty} d\tau \cos\omega\tau \frac{\partial^2 f_2^{\beta\beta}(\tau)}{\partial \tau^2} \tag{58}$$

It is apparent that the connection between the experimental quantity $\varphi(\tau)$ in (56) and the theoretical $\varphi(\tau)$ in (57) is through the observable quantities $f_2^{\beta\beta}(\tau)$ and $f_1^{\beta}(\tau)$. These are seen to be:

$$f_1^{\beta}(\tau) = \int_{D.V.} d^3\underline{x}\, f_1^{\beta}(\underline{x}, \tau) \tag{59}$$

and

$$f_2^{\beta\beta}(\tau) = \int_{D.V.} d^3\underline{x} \int_{D.V.} d^3\underline{x}'\, f_2^{\beta\beta'}(\underline{x}, \underline{x}', \tau) \tag{60}$$

where

$$D.V. \equiv \text{detector volume.} \tag{61}$$

1. The infinite reactor and detector model

The solution of equations (25) to (33) is accomplished directly by Laplace transformation, using the above boundary conditions. In transform space the equations are:

$$f_1^{\beta}(s) = \frac{r_D f_1^{\lambda}}{s^2} \tag{62}$$

$$f_2^{\beta\beta}(s) = \frac{2 r_D f_2^{\beta\lambda}(s)}{s} + \frac{r_D f_1^{\lambda}}{s^2} \tag{63}$$

$$f_2^{\beta\lambda}(s) = \frac{1}{s+r_a}\left\{\frac{r_D(f_2^{\lambda\lambda} - f_1^{\lambda})}{s} + \langle\eta\rangle r_f f_2^{\beta N}(s) + f_1^{\beta}(s)\Gamma\right\} \tag{64}$$

$$f_2^{\beta N}(s) = \frac{1}{s+a_1}\left\{\frac{r_D f_2^{\lambda N}}{s} + f_1^{\beta}(s) S\right\} . \tag{65}$$

Performing the substitution for the stationary quantities and taking the inverse, we find that

$$f_2^{\beta\beta}(t) = A_1 e^{-r_a t} + A_2 e^{-a_1 t} + A_3 t^2 + A_4 t + A_5 \tag{66}$$

$$f_1^{\beta}(t) = A_3^{1/2}\, t \quad , \tag{67}$$

where

$$A_1 = \frac{r_D^2 f_1^N}{r_a^2}\left\{\frac{\langle\eta'^2-\eta\rangle r_f}{r_a} - \frac{\langle\eta\rangle^2 r_f^2 (c_1-a_1)}{r_a (r_a^2-a_1^2)}\right\} \tag{68}$$

$$A_2 = \frac{r_D^2 (c_1-a_1)\langle\eta\rangle^2 r_f^2 f_1^N}{a_1^3 (r_a^2-a_1^2)} \tag{69}$$

$$A_3 = \frac{r_D^2}{r_a^2}\left\{\langle\eta\rangle r_f f_1^N + \Gamma\right\}^2 \tag{70}$$

$$A_4 = \frac{r_D^2}{r_a^2}\left\{\frac{\langle\eta\rangle^2 r_f^2 (c_1-a_1) f_1^N}{a_1^2} + \langle\eta'^2-\eta\rangle r_f f_1^N + \frac{r_a}{r_D}\left[\langle\eta\rangle r_f f_1^N + \Gamma\right]\right\} \tag{71}$$

$$A_5 = -\frac{r_D^2 f_1^N}{r_a^2}\left\{\frac{\langle\eta'^2-\eta\rangle r_f}{r_a} + \frac{\langle\eta\rangle^2 r_f^2 (r_a^3-a_1^3)(c_1-a_1)}{a_1^3 r_a (r_a^2-a_1^2)}\right\} \tag{72}$$

a. The variance

The variance, $V(t)$, is defined as

$$V(t) \equiv f_2^{\beta\beta}(t) - \left[f_1^{\beta}(t)\right]^2 \quad ; \tag{73}$$

and we find:

$$V(t) = A_1 e^{-r_a t} + A_2 e^{-a_1 t} + A_4 t + A_5 \quad . \tag{74}$$

Analysis of the variance:

It is straightforward to show that

$$A_1 + A_2 + A_5 = 0 \quad , \tag{75}$$

and

$$-r_a A_1 - a_1 A_2 + A_4 = A_3^{1/2} \quad . \tag{76}$$

Thus at t = 0 the variance is zero. At small times after t = 0 the variance is equal to $A_3^{1/2} t$. Using (76) it can also be shown that dV/dt is everywhere positive. Therefore the variance exhibits the behavior expected of it. It is zero at t = 0 and positive definite at all times thereafter.

Now let Γ , the gamma source which has been arbitrary up to now, be identified as fission product decay radiation occurring over times greater than one second after fission. It can be shown that in a well-chosen experiment there are negligible fluctuations for the observable gate widths of interest. This is because delayed

fission product radiation is a small fraction of the prompt gamma radiation in this time range, and discrimination for high energy photons is further beneficial for eliminating the effect of Γ because only a minimal number of delayed gammas are born with energies greater than 5 Mev. For the sake of discussion from here on and for the plotting of curves the following numbers will be used, as they are reasonably illustrative of a typical large homogeneous graphite-moderated reactor.

These are:

k = .99

ν_{aN} = 1000 sec^{-1}

ν_f = 396 sec^{-1}

$\langle J \rangle$ = 2.5 prompt neutrons/fission

a_1 = 10 sec^{-1}

$\langle (J-1)^2 \rangle$ = 3.4

$\langle J^2 \rangle$ = 7.4

C_1 = 1950 sec^{-1}

ν_a = 9 x 10^8 sec^{-1}

$\nu_D'^{NaI}$ = 39 x 10^8 sec^{-1} $\equiv \nu_D'$ for 5 Mev gammas

$\langle \eta \rangle^2 \cong$ .04 is a reasonable illustrative value

$\langle \eta \rangle_f \cong$ .03

$\langle \eta'^2 - \eta \rangle$ = .01 .

From equations (67) and (74) the expression for the ratio of the variance to the mean of the charged particles resulting from photon detection events is:

$$\frac{V}{M} = \frac{A_1 e^{-r_a t} + A_2 e^{-a_1 t} + A_4 t + A_5}{A_3^{1/2} t} \quad (77)$$

Using $\Gamma = 0$, $r_a \gg a_1$, and neglecting the appropriate small terms it can be shown that

$$\frac{r_a A_1}{A_3^{1/2}} \cong \frac{r_D}{r_a} \frac{\langle \eta'^2 - \eta \rangle}{\langle \eta \rangle} \quad (78)$$

$$\frac{a_1 A_2}{A_3^{1/2}} \cong \frac{r_D}{r_a} \frac{(c_1 - a_1)\langle \eta \rangle r_f}{a_1^2} \quad (79)$$

$$\frac{A_4}{A_3^{1/2}} \cong 1 + \frac{r_a A_1 + a_1 A_2}{A_3^{1/2}} \quad (80)$$

$$\frac{A_5}{A_3^{1/2}} \cong -\left\{ \frac{1}{a_1} \frac{a_1 A_2}{A_3^{1/2}} + \frac{1}{r_a} \frac{r_a A_1}{A_3^{1/2}} \right\}, \quad (81)$$

and

$$\frac{V}{M} - 1 = \frac{r_D}{r_a}\left\{\frac{\langle \eta'^2 - \eta\rangle}{\langle \eta\rangle}\left[1 - \frac{1 - e^{-r_a t}}{r_a t}\right] + \frac{\langle \eta\rangle r_E (c_1 - a_1)}{a_1^2}\left[1 - \frac{1 - e^{-a_1 t}}{a_1 t}\right]\right\}.$$

(82a)

In most actual instances the first term of (82a) is negligible compared to the second, and one can further reduce (82a) by utilizing (36) and (37) getting:

$$\frac{V}{M} - 1 = \frac{r_D \langle \eta\rangle k^2 \langle J(J-1)\rangle}{r_a \langle J\rangle^2 (1-k)^2}\left[1 - \frac{1 - e^{-a_1 t}}{a_1 t}\right] .$$

(82b)

But from the space averaging procedure pointed out earlier, we find, by considering the photon singlet density, $f_1^{\lambda}(\underline{X})$, which is defined as the expected number of photons per unit volume and is a function of the spatial coordinate, $\underline{X}$, that

$$r_D f_1^{\lambda} = \int_{V_D} d^3\underline{X}\; r_D'(\underline{X})\, f_1^{\lambda}(\underline{X}) \qquad (83a)$$

and

$$r_a f_1^{\lambda} = \int_{V_a} d^3\underline{X}\; r_a(\underline{X})\, f_1^{\lambda}(\underline{X}) \; . \qquad (83b)$$

In the simplified case of a uniform photon distribution in a homogeneous medium with isotropic photon detection and absorption properties it follows that:

$$\frac{r_D}{r_a} = \frac{V_D r_D' f_1^{\lambda}(\underline{x})}{V_a r_a f_1^{\lambda}(\underline{x})} = \frac{V_D r_D'}{V_a r_a} \quad , \tag{84}$$

where

V_D ≡ volume of detector

V_a ≡ reactor volume.

Thus r_D / r_a is seen to act as an efficiency factor. The numerator of equation (84) is simply the count rate of the detected particles. A conservative upper limit on the count rate from a scintillator for the purpose of discussion here is taken to be 10^6 counts per second.

The denominator of equation (84) can be written as

$$V_a r_a f_1^{\lambda}(\underline{x}) = \langle \eta \rangle r_f f_1^{N}(\underline{x}) V_a = \langle \eta \rangle r_f f_1^{N} \, . \tag{85}$$

But

$$r_f f_1^{N} = \frac{P}{\alpha} \quad , \tag{86}$$

where

$\mathcal{P}$ ≡ reactor power (watts)

α ≡ 3×10^{-11} watts per fission/sec.

Then equation (84) becomes

$$\frac{r_D}{r_a} = \frac{\alpha (C.R.)}{\langle \eta \rangle \mathcal{P}} = \frac{3 \times 10^{-10} (C.R.)}{2 \mathcal{P}} \quad , \tag{87}$$

where (C. R.) ≡ resolved count rate.

In the limit of large times

$$\lim_{t \to \infty} \frac{V}{M} - 1 \cong \frac{\alpha (C.R.) \langle J(J-1) \rangle k^2}{\mathcal{P} \langle J \rangle^2 (1-k)^2} \quad . \tag{88}$$

Using the typical numbers for the system parameters given above, it is found that, for $\lim_{t \to \infty} \frac{V}{M} - 1$ to be observable, r_D / r_a must be greater than or equal to 10^{-3}. This implies that in order to see correlation information the reactor power should not exceed approximately . 1 watt for a maximum resolved count rate of 10^6 counts per second. Figure 1 shows $\frac{V}{M} - 1$ plotted versus gate time for the numbers used above.

It is perhaps possible in most instances to resolve the count rate obtained from photon detection events more efficiently by operating on a current mode rather than by resolving individual pulses on a

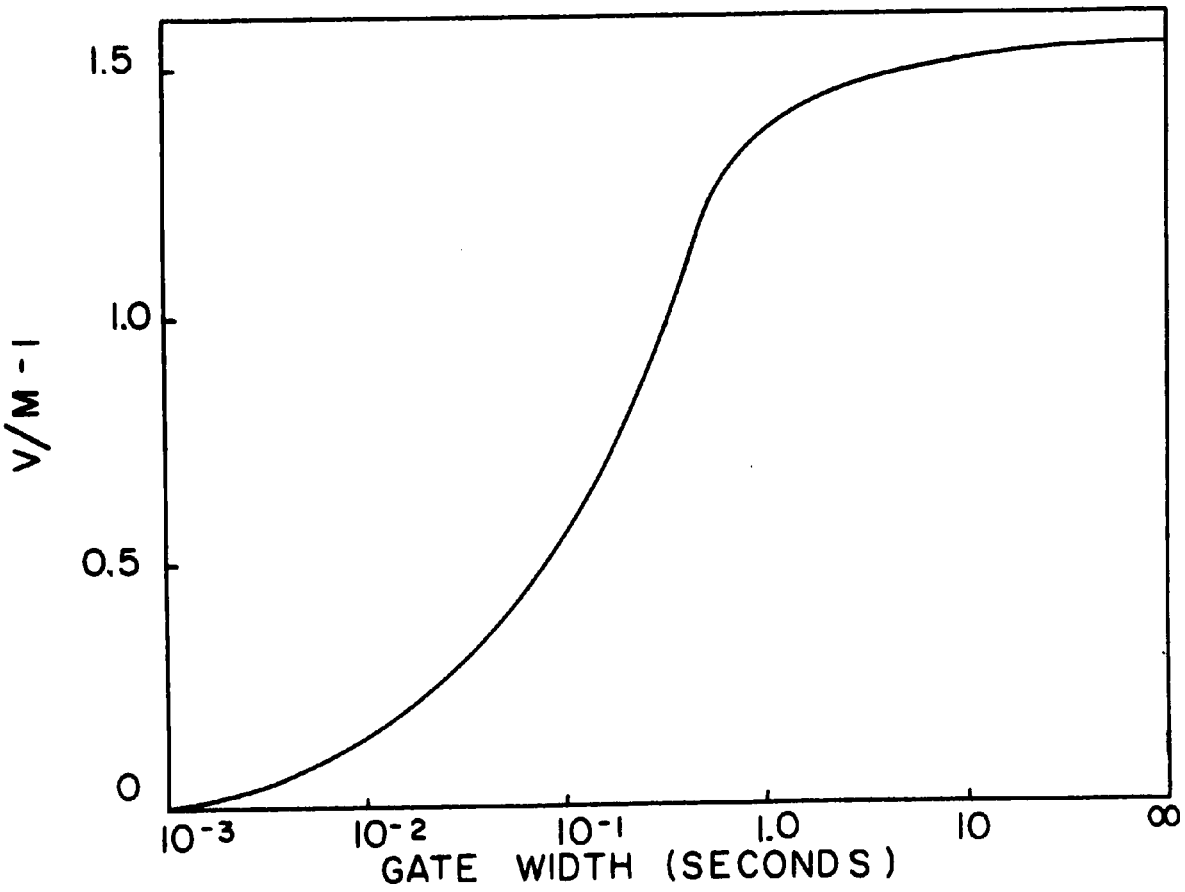


Figure 1. Ratio of Variance to Mean Minus One Versus Gate Width for Photon Detecting Noise Experiment

scaler.* The maximum tolerable reactor power level in these instances probably cannot exceed a kilowatt.

It is clear in principle from this point of view how noise experiments are limited in practice to low power ranges. First, from simple geometric considerations, most experimental arrangements are such that standard-sized detectors can "see" only a portion of the reactor. This results in reduced efficiency except for small special-purpose reactors. Secondly, it is shown above that even if the detector "sees" the entire reactor the resolving time and electronic circuit limitations demand low reactor power levels. The use of noise analysis by photon techniques for determining shutdown reactivity on dirty cores is out of range at the present time because it is possible to combat the pile up of low energy gammas only by sacrificing efficiency with the detectors now available. Also the possibility of monitoring reactors operating at full power is highly questionable. The same limitations obtain in conventional neutron detecting noise experiments, and comparison with the photon analysis can be made.

Now let us compare the conventional type of neutron noise analysis experiment where a BF_3 tube, fission chamber, or a compensated ion chamber is used for neutron detection with the photon detecting experiment discussed above. We start with the corresponding expression for the ratio of the variance to mean of the charged

*Private communication with S. Hanauer.

particles constituting the output of the neutron detector. This expression as obtained elsewhere[16][17] is:

$$\frac{V}{M} - 1 = \frac{r_D (C_1 - a_1)}{a_1^2} \left\{ 1 - \frac{1 - e^{-a_1 t}}{a_1 t} \right\} . \tag{89}$$

In the limit of large times

$$\left[\lim_{t \to \infty} \frac{V}{M} - 1 \right]_N = \frac{r_D (C_1 - a_1)}{a_1^2} \tag{90}$$

where the subscript N denotes the conventional neutron experiment. Equation (90) reduces to

$$\left[\lim_{t \to \infty} \frac{V}{M} - 1 \right]_N = \frac{r_D}{r_f} \frac{\langle J(J-1) \rangle k^2}{\langle J \rangle^2 (1-k)^2} . \tag{91}$$

But as before

$$\frac{r_D}{r_f} = \frac{V_D r_D' f_1^N(\underline{X})}{V_a r_f f_1^N(\underline{X})} = \frac{\alpha (C.R.)_N}{\rho} , \tag{92}$$

Therefore,

$$\left[\lim_{t \to \infty} \frac{V}{M} - 1 \right]_N = \frac{\alpha (C.R.)_N \langle J(J-1) \rangle k^2}{\rho \langle J \rangle^2 (1-k)^2} . \tag{93}$$

The observability of the fluctuations can be compared for the two types of experiments by examining relative amounts by which the variance to mean differs from unity for a given reactor operating at a particular power level.

Define

$$\chi \equiv \left[\lim_{t\to\infty} \frac{V}{M} - 1\right]_N \Big/ \left[\lim_{t\to\infty} \frac{V}{M} - 1\right]_\gamma \quad , \tag{94}$$

where the subscript γ denotes the photon detecting experiment. Then from equations (87), (88), and (91)

$$\chi \equiv \frac{(C.R.)_N}{(C.R.)_\gamma} \quad . \tag{95}$$

In general, scintillators have a higher maximum count rate than can be obtained with standard neutron detectors because of shorter resolving times. In a typical low power experiment, where neither of the respective counters will approach saturation, χ is ideally given by

$$\chi = \left[\frac{r'_{D\gamma} f_1^{\lambda} V_{D\gamma}}{r'_{DN} f_1^{N} V_{DN}}\right]^{-1} \tag{96}$$

or

$$\chi = \left[\frac{r'_{D\gamma}\, r_{aN} \langle \eta \rangle V_{D\gamma} k}{r'_{DN}\, r_a \langle J \rangle V_{DN}} \right]^{-1} . \tag{97}$$

Using a typical value of $r'_{DN} = 553\ \text{sec}^{-1}$ we get

$$\chi = \left[\frac{1}{40} \frac{V_{D\gamma}}{V_{DN}} \right]^{-1} . \tag{98}$$

It should be kept in mind that this quick calculation utilized $\langle \eta \rangle$ which includes prompt gamma contributions from (n, γ) interactions, so that the feasibility of a gamma detecting experiment is further influenced favorably by the presence of high (n, γ) intensities or unfavorably by the absence of (n, γ) interactions in the core. Of course $\langle \eta \rangle$ can be enhanced significantly by lowering the detection threshold to a level $E_o <$ 5 Mev also. Thus it is clear that in the last analysis an optimization of these factors will be necessary in any given experimental situation to really determine the feasibility of the method.

The volumes of the neutron and photon detectors are determined by the effective volume of neutrons or photons which they are capable of "seeing." A neutron detector "sees" neutrons essentially only in that volume which the detector itself occupies physically in the reactor core. In the case of photons which have much greater mean

free paths, the gamma detector is capable of receiving gammas which have traveled considerable distances through the core. This of course implies that the capacity to observe spatially dependent effects is reduced. If a gamma detector is actually placed in the core such that it is a "4π" counter, V_{DI}/V_{DN} may typically be on the order of 50. In this case it could be argued that χ would be on the order of unity. However, the infinite reactor-detector model is misleading if we are intending to place the detector outside the core, as might be proposed in a realistic gamma detecting experiment. In this case χ would be increased further by an appropriate geometric efficiency factor. It is therefore clear that it would not be feasible to have the photon detector placed any great distance from the core due to the effective solid angle considerations. This will be discussed further in the more realistic finite reactor-detector model.

b. The power spectral density.

The power spectral density for photoelectrons is given by

$$\Phi(\omega) = \frac{1}{2} \int_{-\infty}^{\infty} dt \cos \omega t \, \frac{\partial^2 f_2^{\beta\beta}(t)}{\partial t^2} \tag{99}$$

Returning to equation (26) for the computation of the second derivative in (99), and then using (66) and (67) we find that

$$\Phi(\omega) = \frac{r_{DR}^2}{2}\left\{\frac{B_1}{\omega^2+r_a^2} + \frac{B_2}{\omega^2+a_1^2} + B_3\,\delta(\omega)\right\} + \frac{r_{DR}\,B_4}{2} \quad , \tag{100}$$

where

$$B_1 \equiv \langle\eta'^2-\eta\rangle r_f f_1^N - \frac{\langle\eta\rangle^2 r_f^2 (c_1-a_1) f_1^N}{r_a^2 - a_1^2} \tag{101a}$$

$$B_2 \equiv \frac{\langle\eta\rangle^2 r_f^2 (c_1-a_1) f_1^N}{r_a^2 - a_1^2} \tag{101b}$$

$$B_3 \equiv 2\left\{\frac{\langle\eta\rangle r_f f_1^N}{r_a} + \frac{\Gamma}{r_a}\right\}^2 \tag{101c}$$

$$B_4 \equiv \frac{\langle\eta\rangle r_f f_1^N}{r_a} + \frac{\Gamma}{r_a} \tag{101d}$$

Again using $\Gamma = 0$; $r_a >> a_1$ and neglecting appropriate small quantities

$$B_1 \cong \langle\eta'^2-\eta\rangle r_f f_1^N \tag{102}$$

$$B_z \cong \frac{\langle \eta \rangle^2 r_f^2 (c_1 - a_1) f_1^N}{r_a^2} \quad . \tag{103}$$

Then applying equation (71) for $r_{D\gamma}/r_a$ we have

$$\Phi(\omega) \cong \frac{\langle \eta \rangle r_{D\gamma} r_f f_1^N}{2 r_a} \left\{ 1 + \frac{\alpha (C.R.)_\gamma}{\rho} \left[\frac{r_f (c_1 - a_1)}{\omega^2 + a_1^2} + \right. \right.$$

$$\left. \left. + \frac{\langle \eta'^2 - \eta \rangle}{\langle \eta \rangle^2} \frac{r_a^2}{\omega^2 + r_a^2} \right] \right\} . \tag{104}$$

Using the same typical numbers as before for the parameters above, $\Phi(\omega)$ (with constant term subtracted off) is plotted in decibels versus the frequency ω in Figure 2. It is seen here that the information of interest from the power spectral density is obtained by analysis in the frequency range from 1 cps to 10^4 cps. Clearly then delayed gamma radiation from fission product decay poses no particular problem to the interpretation of power spectrum measurements, because it has been shown that there is negligible gamma emission in the time interval following fission which corresponds to the frequency range of prime interest here[2].

Furthermore, reduction of (104) gives

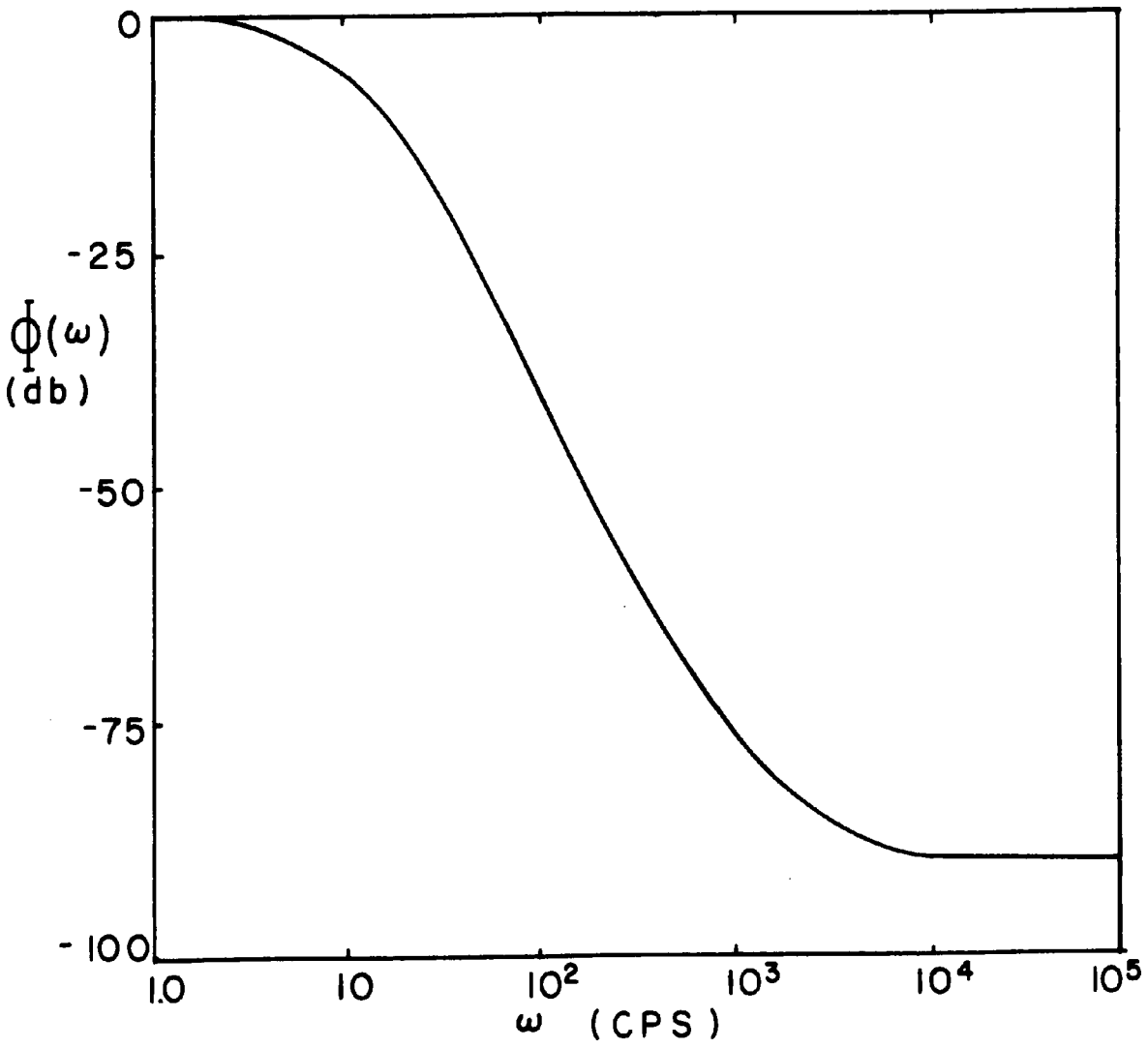


Figure 2. The Power Spectral Density Versus Frequency for Photon Detecting Noise Experiment

$$\Phi(\omega) = \frac{\langle \eta \rangle r_{DI} r_c f_1^N}{2 r_a} \left\{ 1 + \frac{\alpha(C.R.)_I}{P} \left[\frac{k^2 \langle J(J-1) \rangle}{\langle J \rangle^2 (1-k)^2} \frac{a_1^2}{\omega^2 + a_1^2} + \right. \right.$$

$$\left. \left. + \frac{\langle \eta'^2 - \eta \rangle}{\langle \eta \rangle^2} \frac{r_a^2}{\omega^2 + r_a^2} \right] \right\} . \qquad (105)$$

Summarizing Remarks

The theory which has been developed above for reactor correlation studies by photon detection indicates that in principle information relevant to dynamic reactor parameters may be obtained in some instances as efficiently as in neutron detecting noise experiments. It is seen that the stochastic information of the system resides in the photon distribution of the reactor as well as in the neutron distribution. It appears that for the present these observations will be limited to clean cores as is the case in neutron noise analysis as well.

The fact that photons may in principle be used for noise analysis as well as neutrons may become more apparent by examining the following expressions for the ratio of the variance to mean and for the power spectral densities for both the gamma detecting experiment and for the neutron experiment.

For Gammas:

$$\Phi(\omega) = \frac{\langle\eta\rangle r_{DS} r_f f_1^N}{2 r_a}\left\{1 + \frac{\alpha(C.R.)_\gamma}{\rho}\left[\frac{k^2\langle J(J-1)\rangle}{\langle J\rangle^2(1-k)^2}\,\frac{a_1^2}{\omega^2+a_1^2} + \right.\right.$$

$$\left.\left. + \frac{\langle\eta'^2-\eta\rangle}{\langle\eta\rangle^2}\,\frac{r_a^2}{\omega^2+r_a^2}\right]\right\} . \qquad (106)$$

Equation (82a) reduces to:

$$\frac{V}{M} = 1 + \frac{\alpha(C.R.)_\gamma}{\rho}\left\{\frac{k^2\langle J(J-1)\rangle}{\langle J\rangle^2(1-k)^2}\left[1 - \frac{1-e^{-a_1 t}}{a_1 t}\right] + \right.$$

$$\left.\frac{\langle\eta'^2-\eta\rangle}{\langle\eta\rangle^2}\left[1 - \frac{1-e^{-r_a t}}{r_a t}\right]\right\} . \qquad (107)$$

For Neutrons:

These expressions may be obtained from (16).

$$\Phi(\omega) = \frac{r_{DN} f_1^N}{2}\left\{1 + \frac{\alpha(C.R.)_N}{\rho}\,\frac{k^2\langle J(J-1)\rangle}{\langle J\rangle^2(1-k)^2}\,\frac{a_1^2}{\omega^2+a_1^2}\right\} , \qquad (108)$$

and equation (89) reduces to:

$$\frac{V}{M} = 1 + \frac{\alpha(C.R.)_N}{\rho}\,\frac{k^2\langle J(J-1)\rangle}{\langle J\rangle^2(1-k)^2}\left[1 - \frac{1-e^{-a_1 t}}{a_1 t}\right] . \qquad (109)$$

It is abundantly clear by comparison of the expressions above that observation of reactor fluctuations by photon observation in the range of gate times and frequencies that are practical is equivalent to the observation by neutron detection to within an exceedingly small term in each case if "4π" counters are used in each case.

A few general remarks can be made regarding the ramifications of some of the assumptions that have been made in order to formulate a reasonable working model that is at the same time readily amenable to straightforward analysis. The applicability of the results that have been obtained appears severely limited by the employment of kinetic equations which contain no explicit information about the time-phase space coupling that chracterizes neutron distributions in real systems. The justification for such a simplified description of singlet densities is usually accomplished in the context of bare, homogeneous, thermal systems executing small temporal variations throughout which space-time separability of these densities is realized to good approximation. However, the analysis of noise experiments requires detailed consideration of doublet densities, and the criteria which suggest the utility of the "point reactor" kinetic equations for the description of the singlet densities are no guarantee that similar simplifications are justified in this case. However, there is one practical situation in which the use of "point reactor" kinetics to describe both singlet and doublet densities has been demonstrated to be valid, provided the parameters entering the equations are appropriately interpreted.

Examples are small core, water moderated swimming pool reactors, as has been demonstrated both experimentally[17][18] and theoretically[10][19]. The point is that, in these reactors, the two-point space dependence of the neutron doublet density approximately factors into the product of lowest mode reactor eigenfunctions. In consequence, the "point reactor" kinetic equations become applicable provided the lifetime and reactivity parameters entering therein are appropriately corrected for fast and thermal leakage effects[10][19]. These considerations are important to the analysis of neutron noise experiments which employ neutron detectors, and they apply with equal force to the present analysis of neutron noise measurements relying on photon detectors. These considerations become more apparent in the next section.

2. The finite reactor and detector model.

a. The power spectral density.

We now write the power spectral density as:

$$\Phi(\omega) = \frac{1}{2} \int_{-\infty}^{\infty} dt \cos \omega t \, \frac{\partial^2 V^{\beta\beta'}(t)}{\partial t^2} \tag{110}$$

(valid for non zero frequencies).

The quantity $V^{\beta\beta'}(t)$ is the variance of photoelectrons defined by

$$\int_{(D.V.)_1} d^3\underline{x} \int_{(D.V.)_2} d^3\underline{x}' \left\{ f_2^{\beta\beta'}(\underline{x},\underline{x}',t) - f_1^{\beta}(\underline{x},t) f_1^{\beta'}(\underline{x}',t) \right\} . \tag{111}$$

The equations for the variances that are needed are obtained directly from our previously reduced multiplet equations. They are

$$\frac{\partial V^{\beta\beta'}(\underline{x},\underline{x}',t)}{\partial t} = \Big\{ \Delta V^{\lambda\beta'}(\underline{x},\underline{x}',t) + \Delta' V^{\beta\lambda'}(\underline{x},\underline{x}',t) + \delta(\underline{x}-\underline{x}')\,\Delta f_1^{\lambda}(\underline{x}) \Big\} H(t) \tag{112}$$

and by differentiating

$$\frac{\partial^2 V^{\beta\beta'}(\underline{x},\underline{x}',t)}{\partial t^2} = \left\{ \Delta \frac{\partial V^{\lambda\beta'}(\underline{x},\underline{x}',t)}{\partial t} + \Delta' \frac{\partial V^{\beta\lambda'}(\underline{x},\underline{x}',t)}{\partial t} \right\} H(t) + \delta(\underline{x}-\underline{x}')\,\Delta f_1^{\lambda}(\underline{x})\,\delta(t) . \tag{113}$$

To get this equation we have used the properties of the step function and the initial conditions given as

$$V^{\beta\beta'}(0) = V^{\beta\lambda'}(0) = V^{\lambda\beta'}(0) = V^{\beta N'}(0) = V^{N\beta'}(0) = 0 \,.$$

(114)

In like manner we have

$$\left[\frac{\partial}{\partial t} + B_\gamma\right] V^{\lambda\beta'}(\underline{x}, \underline{\Omega}; \underline{x}'; t) = \left\{\Delta' V^{\lambda\lambda'}(\underline{x}, \underline{\Omega}; \underline{x}') + \right.$$

$$\left. + \frac{P_\gamma}{4\pi} V^{N\beta'}(\underline{x}, \underline{x}', t) - \delta(\underline{x} - \underline{x}') r_D f_1^{\lambda'}(\underline{x}, \underline{\Omega}) \right\} H(t) \,,$$

(115)

and $V^{\beta\lambda'}(\underline{x}; \underline{x}', \underline{\Omega}'; t)$ is obtained by interchanging arguments.

We also have

$$\left[\frac{\partial}{\partial t} + B_N\right] V^{N\beta'}(\underline{x}, \underline{x}', t) = \Delta' V^{N\lambda'}(\underline{x}, \underline{x}') H(t) \,.$$

(116)

If we apply the consistent P-1 procedure to reduce the neutron equations, we can write the neutron Boltzmann operator, B_N, as

$$B_N f^N(\underline{x}) = \left[a_1 - D_1 \nabla^2\right] f^N(\underline{x}) \,,$$

(117)

where

$$D_1 \equiv \langle v \rangle^2 / 3 b_1 \tag{118}$$

$\langle v \rangle \equiv$ mean speed of neutrons (119)

$$b_1 \equiv r_{aN} + [1 - \langle \mu \rangle] r_s = r_t - \langle \mu \rangle r_s \tag{120}$$

$\langle \mu \rangle \equiv$ first angular moment of the neutron scattering frequency. (121)

The details concerning the reduction of the neutron equations have been given careful attention by Osborn and Natelson[10] and others[19], and will not be belabored by us at this point. The equation for $V^{\beta N'}(\underline{X}, \underline{X}', t)$ is obtained by interchanging arguments.

The solutions for these variances can be obtained by Fourier-Laplace transformation.

$$V^{\lambda\beta'}(\underline{k}, \underline{\Omega}; \underline{X}'; s) = \frac{\Delta' V^{\lambda\lambda'}(\underline{k}, \underline{\Omega}; \underline{X}') - e^{-i\underline{k}\cdot\underline{X}'} f_1^{\lambda}(\underline{X}', \underline{\Omega})}{ic\underline{k}\cdot\underline{\Omega} + r_a} \tag{x}$$

$$(x)\left[\frac{1}{s} - \frac{1}{s + ic\underline{k}\cdot\underline{\Omega} + r_a}\right] + \frac{P_\gamma}{4\pi} \frac{V^{N\beta'}(\underline{k}; \underline{X}'; s)}{s + ic\underline{k}\cdot\underline{\Omega} + r_a} \Bigg) \tag{122}$$

where it is noted that $\underline{k}$ is the Fourier variable from here on.

$$V^{\lambda\beta'}(\underline{k},\underline{\Omega};\underline{X}';s) \equiv \mathcal{FL}\left\{V^{\lambda\beta'}(\underline{X},\underline{\Omega};\underline{X}';t)\right\} =$$

$$= \int_{t=0}^{\infty} dt\, e^{-st} \int d^3k\, e^{-i\underline{k}\cdot\underline{X}}\, V^{\lambda\beta'}(\underline{X},\underline{\Omega};\underline{X}';t) .$$

(123)

If now we Fourier-Laplace transform equation (116) and let

$$b \equiv a_1 + D_1 k^2 \quad , \tag{124}$$

we get:

$$V^{N\beta'}(\underline{k},\underline{X}',s) = \frac{\Delta' V^{N\lambda'}(\underline{k},\underline{X}')}{s(s+b)} \quad . \tag{125}$$

Then going back to equation (122) and taking the inverse Laplace transformation, it can be shown that upon inversion the first term which is proportional to $\left[\frac{1}{s} - \frac{1}{s+ic\,\underline{k}\cdot\underline{\Omega}+\nu_a}\right]$ in equation (122) will not contribute to the power spectral density at observable frequencies and can therefore be neglected. This is because the first term in brackets gives something proportional to $\delta(\omega)$, and the second term will give something proportional to $\frac{1}{\omega^2+\nu_a^2}$ which is constant over the observable frequency range of $\Phi(\omega)$.

Substituting (125) into the remaining expression for

$V^{\lambda\beta'}(\underline{k}, \underline{\Omega}; \underline{X}', s)$ we have

$$sV^{\lambda\beta'}(\underline{k}, \underline{\Omega}; \underline{X}'; s) = \frac{P_\gamma \Delta' V^{N\lambda'}(\underline{k}, \underline{X}')}{4\pi (s + ic\underline{k}\cdot\underline{\Omega} + r_a)(s+b)} \quad (126)$$

Using $V^{\lambda\beta'}(\underline{k}, \underline{\Omega}; \underline{X}'; t=0) = 0$ the Laplace inverse of (126) gives

$$\frac{\partial V^{\lambda\beta'}(\underline{k}, \underline{\Omega}; \underline{X}'; t)}{\partial t} = \frac{P_\gamma \Delta' V^{N\lambda'}(\underline{k}, \underline{X}') e^{-bt}}{4\pi (ic\underline{k}\cdot\underline{\Omega} + r_a)} \quad (127)$$

where we have neglected:

(1) terms proportional to $e^{-r_a t}$

(2) b compred to r_a .

To take the Fourier inverse of (127), we use the relationship

$$\frac{1}{ic\underline{k}\cdot\underline{\Omega} + r_a} = \int_{p=0}^{\infty} dp\, e^{-[ic\underline{k}\cdot\underline{\Omega} + r_a]p} \quad (128)$$

It can be readily verified that the integrand of (128) vanishes at $p = \infty$ as required.

Then

$$\frac{\partial V^{\lambda\beta'}(\underline{X},\underline{\Omega};\underline{X}';t)}{\partial t} = \frac{P_\beta \Delta' e^{-bt}}{4\pi(2\pi)^3}\int_{p=0}^{\infty} dp \int_{-\infty}^{\infty} d^3k \int_{-\infty}^{\infty} d^3\underline{X}''\, e^{-i\underline{k}\cdot\underline{X}''} \quad (*)$$

$$(*)\, V^{N\lambda'}(\underline{X}'', \underline{X}')\, e^{i\underline{k}\cdot[\underline{X} - cp\underline{\Omega}]}\, e^{-r_a p} \,,$$

(129)

which can be written as

$$\frac{\partial V^{\lambda\beta'}(\underline{X},\underline{\Omega};\underline{X}';t)}{\partial t} = \frac{P_\gamma \Delta' e^{-bt}}{4\pi}\int_{p=0}^{\infty} dp \int_{-\infty}^{\infty} d^3\underline{X}''\, \delta(\underline{X} - \underline{X}'' - cp\underline{\Omega})(*)$$

$$(*)\, V^{N\lambda'}(\underline{X}'', \underline{X})\, e^{-r_a p} \,.$$

(130)

If we let

$$\underline{X} - \underline{X}'' \equiv \underline{X}''' \tag{131}$$

and

$$\delta(\underline{X}''' - cp\underline{\Omega}) = \frac{1}{C}\,\frac{\delta(\frac{X'''}{C} - p)\,\delta(\hat{\Omega}_{X'''} - \underline{\Omega})}{|X'''|^2} \,, \tag{132}$$

we finally get

$$\frac{\partial V^{\lambda\lambda'}(\underline{X},\underline{\Omega};\underline{X}';t)}{\partial t} = \frac{P_\gamma \Delta' e^{-bt}}{4\pi} \int_{R=0}^{\infty} \frac{dR}{c}\, e^{-R/\lambda_a} V^{N\lambda'}(\underline{X}-R\underline{\Omega},\underline{X}').$$

(133)

We have replaced $|\underline{X}'''|$ by R and used $\lambda_a = c/r_a$.

The equation for $V^{N\lambda'}(\underline{X}-R\underline{\Omega};\underline{X}',\underline{\Omega}')$ is:

$$\left[B_N + B_\gamma'\right] V^{N\lambda'}(\underline{X}-R\underline{\Omega};\underline{X}',\underline{\Omega}') = \frac{P_\gamma}{4\pi} V^{NN'}(\underline{X}-R\underline{\Omega};\underline{X}') -$$

$$-\delta(\underline{X}-R\underline{\Omega}-\underline{X}')\frac{P_\gamma}{4\pi} f_1^N(\underline{X}-R\underline{\Omega}).$$

(134)

Recalling that $B_N f^N$ becomes bf^N upon averaging over energy and direction, and that $b \ll r_a$, the solution to (134) is readily found to be:

$$V^{N\lambda'}(\underline{X}-R\underline{\Omega};\underline{X}',\underline{\Omega}') = \int_{R'=0}^{\infty} \frac{dR'}{c} e^{-R'/\lambda_a} \left\{ \frac{P_\gamma'}{4\pi} V^{NN'}(\underline{X}-R\underline{\Omega};\underline{X}'-R'\underline{\Omega}') - \right.$$

$$\left. -\delta(\underline{X}-R\underline{\Omega}-(\underline{X}'-R'\underline{\Omega}'))\frac{P_\gamma'}{4\pi} f_1^N(\underline{X}-R\underline{\Omega}) \right\}.$$

(135)

So we finally have:

$$\frac{\partial V^{\lambda\beta'}(\underline{X},\underline{\Omega};\underline{X}';t)}{\partial t} = \frac{P_\gamma P_\gamma'}{(4\pi)^2}\Delta' e^{-bt}\int_{R=0}^{\infty}\frac{dR}{c}\,e^{-R/\lambda_a}\int_{R'=0}^{\infty}\frac{dR'}{c}\,e^{-R'/\lambda_a}$$

$$\sum_{(\alpha)}\left\{V^{NN'}(\underline{X}-R\underline{\Omega};\underline{X}'-R'\underline{\Omega}') - \delta(\underline{X}-R\underline{\Omega}-(\underline{X}'-R'\underline{\Omega}'))f_1^N(\underline{X}-R\underline{\Omega})\right\}H(t).$$

(136)

We have now solved for $\frac{\partial V^{\lambda\beta'}(\underline{X};\underline{X}';t)}{\partial t}$ and therefore for $\frac{\partial^2 V^{\beta\beta}(\underline{X},\underline{X}',t)}{\partial t^2}$ in terms of the neutron variance and the neutron singlet density, which have been worked out in detail in the work of Natelson, Osborn, and Shure[19]. They found:

$$V^{NN'}(\underline{X}-R\underline{\Omega};\underline{X}'-R'\underline{\Omega}') = \sum_{n,m,i} C_{inm}\frac{\langle J(J-1)\rangle r_f A_i^N \psi_n(\underline{X}-R\underline{\Omega})\psi_m(\underline{X}'-R'\underline{\Omega}')}{2a_1 + D_1(B_n^2+B_m^2)} +$$

$$+\delta(\underline{X}-R\underline{\Omega}-(\underline{X}'-R'\underline{\Omega}'))f_1^N(\underline{X}-R\underline{\Omega}),$$

(137)

where

$$C_{inm} = \int_{R.V.} d^3X\,\psi_i(\underline{X})\psi_n(\underline{X})\psi_m^\dagger(\underline{X})$$

(138a)

and

$$f_1^N(\underline{X},t) = \sum_n^{\infty} A_n(t)\,\psi_n(\underline{X}) \quad .$$

(138b)

By using (136) and (137) in (113)

$$\frac{\partial^2 V^{\beta\beta'}(t)}{\partial t^2} = \int_{(D.V.)_1} d^3X \int_{(D.V.)_2} d^3X' \left\{ \frac{P_\gamma P_\delta'}{(4\pi)^2} \Delta\Delta' e^{-bt} \int_{R=0}^{\infty} \frac{dR}{C} \int_{R'=0}^{\infty} \frac{dR'}{C} e^{-R/\lambda_a} e^{-R'/\lambda_a} \right.$$

$$\cdot \left[2 \sum_{n,m,i} C_{inm} \frac{\langle J(J-1)\rangle r_f A_i^N \psi_n(\underline{X}-R\underline{\Omega})\,\psi_m(\underline{X}'-R'\underline{\Omega}')}{2a_1 + D_1(B_n^2 + B_{m'}^2)} \right] H(t) +$$

$$\left. + \delta(\underline{X}-\underline{X}') \frac{\Delta P_\delta}{4\pi} \int_{R=0}^{\infty} \frac{dR}{C} e^{-R/\lambda_a} f_1^N(\underline{X}-R\underline{\Omega})\,\delta(t) \right\} .$$

(139)

To evaluate this expression further, consider detectors 1 and 2 to be placed outside the reactor core. The set of points $\{\underline{X}_1\}$ define the volume occupied by detector 1, and the set of points $\{\underline{X}_2\}$ correspondingly obtain for detector 2. Let a thickness $\bar{z}$ of moderator, say, water, lie between the detector and the core. The detector will be able to "see" photons from within some given volume, V_S, of the reactor core and moderator as shown in Figure 3.

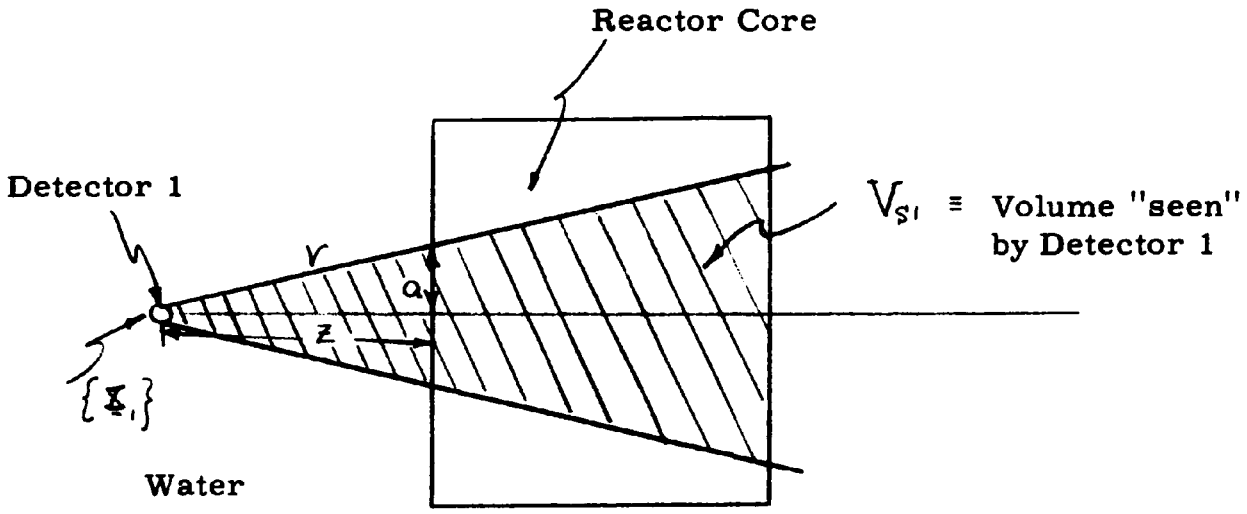


Figure 3. Diagram of Finite Reactor, Finite Detector System

If we let the set of directional vectors extending from points $\{\underline{X}_1\}$ into V_{S1} be denoted by $\{\underline{\Omega}_1\}$, the detection rate has the following property:

$$r_{D1}(\underline{X}) = r_{D1} \quad \text{for } \underline{X} \text{ in } \{\underline{X}_1\} \text{ and for photons along vectors } \{\underline{\Omega}_1\}$$

$$= 0 \quad \text{otherwise} \tag{140}$$

If we consider the detection rate to be effectively constant over the photon energies of interest, we can write for detector 1, using (43):

$$\Delta_1 f^{\lambda}(\underline{X}) = \int d^3k \; r_{D1}(\underline{X}) f_1^{\lambda}(\underline{X}, \underline{k}) \tag{141a}$$

or

$$\Delta_1 f^{\lambda}(\underline{X}) = r_{D1}(\underline{X}) \int_{\{\underline{\Omega}_1\}} d\Omega\, f^{\lambda}(\underline{X}, \underline{\Omega}) \tag{141b}$$

and likewise for detector 2

$$\Delta_2 f^{\lambda}(\underline{X}') = r_{D2}(\underline{X}') \int_{\{\underline{\Omega}_2\}} d\Omega'\, f^{\lambda}(\underline{X}', \underline{\Omega}') \ . \tag{142}$$

From here on we let $V_{D1} = V_{D2} = V_D$ and $r_{D1} = r_{D2} = r_D$, and for convenience each detector is assumed to "see" the same solid angle.

The power spectral density can then be written as:

$$\Phi(\omega) = \frac{1}{2} \int_{(D.V.)_1} d^3X \int_{(D.V.)_2} d^3X' \, \frac{r_D(\underline{X}) \langle \eta \rangle r_f}{C} \left\{ \frac{2\, r_D(\underline{X}') \langle \eta \rangle r_f}{C} \int_{R=0}^{\infty} dR \int_{\{\underline{\Omega}_1\}} d\Omega^{(x)} \right.$$

$$^{(x)} \frac{e^{-R/\lambda_a}}{4\pi} \int_{R=0}^{\infty} dR' \int_{\{\underline{\Omega}_2\}} d\Omega' \, \frac{e^{-R'/\lambda_a}}{4\pi} \sum_{n,m,i} \frac{C_{inm} \langle J(J-1) \rangle r_f A_i^N \psi_n(\underline{X} - R\underline{\Omega}) \psi_m(\underline{X}' - R'\underline{\Omega}')}{2a_1 + D_1(B_n^2 + B_m^2)} {}^{(x)}$$

$$\left. {}^{(x)} \frac{b}{\omega^2 + b^2} + \delta(\underline{X} - \underline{X}') \int_{R=0}^{\infty} dR \int_{\{\underline{\Omega}_1\}} d\Omega \, \frac{e^{-R/\lambda_a}}{4\pi} f_1^N(\underline{X} - R\underline{\Omega}) \right\} . \tag{143}$$

Rather than attempt an exact solution for expression (143), which would require numerical techniques and would not be particularly illuminating, we will instead deduce an approximate analytic solution. Let us first work on the second (and simplest) integral in equation (143). We recognize that upon multiplying numerator and denominator by R^2 that

$$\phi^{\gamma}(\underline{x}) \equiv \int_{V_{S1}} d^3R \langle \eta \rangle r_f f_1^N(\underline{x} - R\underline{\Omega}) \frac{e^{-R/\lambda_a}}{4\pi R^2} \tag{144}$$

represents the flux of photons arriving at $\underline{x}$, having been born in that part of the core that the detector is capable of "seeing." We now proceed by utilizing a simplified model that is amenable to solution by a standard shielding calculation[20][21].

Assume:

(1) The density of neutrons is taken to be constant in V_S of the reactor core. $\overline{[f_1^N(\underline{x})]}_{V_S} \equiv (f_1^N)_S$ denotes a constant (averaged) density in V_S.

(2) Photons in the energy range of interest are born isotropically in the core, and it is assumed that none are produced in the moderator.

(3) $\lambda_a = \lambda_{ac}$ in the core

$\lambda_a = \lambda_{am}$ in the moderator

(4) The thickness of the core is on the order of several

photon mean free paths.

We now use

$$\langle\eta\rangle r_f (f_1^N)_S \equiv S_V = \text{number of gammas born per unit volume per sec} \tag{145}$$

to develop an approximate equivalent isotropic plane source of photons at the core moderator interface. This is denoted by ϕ_i, and

$$\phi_i \cong \frac{S_V \lambda_{ac}}{2} = \frac{c\langle\eta\rangle r_f (f_1^N)_S}{2 r_a} \tag{146}$$

Thus we are effectively viewing at $\underline{X}$ a constant isotropic source of photons from a finite plane located a distance z along the normal from $\underline{X}$ to the plane source. See Figure 3.

The solution for $\phi^\gamma(\underline{X})$ is given by

$$\phi^\gamma(\underline{X}) \simeq 2\pi \int_{r=z}^{(z^2+a^2)^{1/2}} r\,dr\,\phi_i \frac{e^{-r/\lambda_{am}}}{4\pi r^2} \tag{147}$$

or letting $x \equiv r/\lambda_{am}$ we have

$$\phi^\gamma(\underline{X}) \simeq \frac{\phi_i}{2} \int_{x=z/\lambda_{am}}^{(z^2+a^2)^{1/2}/\lambda_{am}} \frac{e^{-x}}{x}\,dx \tag{148}$$

But note that the integral in (148) is closely related to the $n=1$ member of the set of exponential integral functions defined by

$$E_n(z/\lambda_{am}) = (z/\lambda_{am})^{n-1} \int_{x=z/\lambda_{am}}^{\infty} \frac{e^{-x}}{x^n}\, dx \quad . \tag{149}$$

The values for $E_n(x)$ are tabulated in references (20) and (21). Therefore we write equation (148) as

$$\phi^{r}(\underline{x}) \cong \frac{\Phi_i}{2}\left\{ \int_{x=z/\lambda_{am}}^{\infty} \frac{e^{-x}}{x}\, dx - \int_{x=(z^2+a^2)^{1/2}/\lambda_{am}}^{\infty} \frac{e^{-x}}{x}\, dx \right\} \tag{150}$$

or

$$\phi^{\gamma}(\underline{x}) \cong \frac{\Phi_i}{2}\left\{ E_1(z/\lambda_{am}) - E_1([z^2+a^2]^{1/2}/\lambda_{am}) \right\} \equiv \Phi_i\, \Omega_1(z,a). \tag{151}$$

The factor $\Omega_1(z,a)$ is the "solid angle efficiency factor."

It was pointed out in reference (19) that for small reactors whose dimensions are such that they do not greatly exceed the migration length of neutrons in the reactor, the zeroth reactor mode will dominate the summation in (143). Then corresponding to detector 1 we have

$$\left(f_1^N\right)_{S1} = \overline{A_o(\psi_{o1})_S} = A_o\,\overline{(\psi_{o1})_S} \quad , \tag{152}$$

where A_o is just a number independent of spatial co-ordinates.

In the summation of (143) replace

$$\psi_n(\underline{x} - R\underline{\Omega}) \quad \text{by} \quad \overline{(\psi_{o1})_S} \qquad \text{for } \underline{x} \text{ in } \{\underline{x}_1\} \text{ and } \underline{\Omega} \text{ in } \{\underline{\Omega}_1\}$$

and

$$\psi_m(\underline{x}' - R'\underline{\Omega}') \quad \text{by} \quad \overline{(\psi_{o2})_S} \qquad \text{for } \underline{x}' \text{ in } \{\underline{x}_2\} \text{ and } \underline{\Omega}' \text{ in } \{\underline{\Omega}_2\} \; .$$

Then

$$\Phi(\omega) = \frac{1}{2}\,\frac{\langle\eta\rangle r_f r_D V_D}{r_a}\,A_o\overline{(\psi_{o1})_S}\,\Omega_1(z,a)\left\{A(D_1 \cap D_2) + \right.$$

$$\left. + \frac{r_D\langle\eta\rangle r_f V_D}{r_a}\,\Omega_0(z,a)\,\frac{\langle J(J-1)\rangle r_f C_{000}\,\overline{(\psi_{o2})_S}}{\omega^2 + b^2}\right\} . \tag{153}$$

In this equation we have used $A(D_1 \cap D_2)$ to represent the relative overlap of the two detectors. Of course the extreme values of this function are unity for complete overlap (or a single detector experiment) and zero for no overlap whatsoever.

We have used

$$b = a_1 + D_1 B_o^2 \quad . \tag{154}$$

We can write a disadvantage factor for the densities that correspond to detector 1 as:

$$\mathcal{D}_1 \equiv \frac{(f_1^N)_{S1}}{(f_1^N)_R} = \frac{(\overline{\psi_{01}})_S}{(\overline{\psi_0})_R} \quad . \tag{155}$$

Also

$$\mathcal{D}_1 = \frac{(N_1^N)_{S1}}{(N_1^N)_R} \frac{V_R}{V_{S1}} \quad , \tag{156}$$

where

$(f_1^N)_R \equiv$ the neutron singlet density appropriately averaged over the entire reactor (157)

$(N_1^N)_{S1} \equiv$ number of neutrons in the core volume seen by the detector 1 (158)

$(N_1^N)_R \equiv$ total number of neutrons in the reactor . (159)

Now

$$C_{000}(\overline{\psi_{02}})_S = C_{000}\mathcal{D}_2(\overline{\psi_{02}})_R = C_{000}\mathcal{D}_2(\overline{\psi_0})_R \tag{160}$$

To evaluate $C_{000}(\overline{\psi_0})_R$, let us recall that

$$C_{000} \equiv \int_{R.V.} d^3\underline{X}\ \psi_0(\underline{X})\psi_0(\underline{X})\psi_0^t(\underline{X}) \quad . \tag{161}$$

From the orthonormality of the reactor modes we can see that $\psi_o(\underline{x})$ is of the form

$$\psi_o(\underline{x}) = \frac{W(\underline{x})}{V_R^{1/2}} \quad . \tag{162}$$

For a cubic reactor, as an example, $W(\underline{x})$ is just the product of three cosine terms.

Thus

$$\int_{R.V.} d^3x' \, \psi_o(\underline{x}' - R'\underline{\Omega}') = \int_{R.V.} d^3x' \, \frac{W(\underline{x}')}{V_R^{1/2}} \tag{163}$$

or

$$V_R \overline{(\psi_o')}_R = \frac{\overline{W(\underline{x}')}\, V_R}{V_R^{1/2}} \quad . \tag{164}$$

Therefore

$$\overline{(\psi_o')}_R = \frac{\overline{W(\underline{x}')}}{V_R^{1/2}} = \left(\frac{4}{\pi}\right)^3 \frac{1}{V_R^{1/2}} \quad . \tag{165}$$

In the same manner we can find

$$C_{000} = \frac{\mathcal{K}}{V_R^{1/2}} = \left(\frac{8}{3\pi}\right)^3 \frac{1}{V_R^{1/2}}$$

for a cubic reactor. (166)

Utilizing these results

$$C_{000}\left(\overline{\psi_0'}\right)_R \approx \frac{1}{V_R} \tag{167}$$

which leads to

$$\Phi(\omega) = \frac{1}{2}\frac{\langle\eta\rangle r_f r_D V_D (N_1^N)_R \delta_1 \Omega_2(z,a)}{r_a V_R}\left\{ A(D_1 \cap D_2) + \right.$$

$$\left. + \frac{\langle\eta\rangle r_f r_D V_D}{r_a V_R}\delta_2 \Omega_1(z,a)\frac{\langle J(J-1)\rangle r_f}{\omega^2 + b^2}\right\} . \tag{168}$$

It can be seen that for detector 1 as an example

$$\frac{\langle\eta\rangle r_f r_D V_D (N_1^N)_R \delta_1 \Omega_2(z,a)}{r_a V_R} = (C.R.)_{\gamma 1} . \tag{169}$$

Also, using (156) for δ_2 and multiplying numerator and denominator by r_f, we see that

$$\frac{\langle\eta\rangle r_f r_D V_D \delta_2 \Omega_2(z,a)}{r_a V_R} = \frac{\alpha\, r_f (C.R.)_{\gamma 2}}{\rho} . \tag{170}$$

Then we can finally write the power spectral density as:

$$\Phi(\omega) = \frac{(C.R.)_{\gamma 1}}{2}\left\{A(D_1 \cap D_2) + \frac{\alpha(C.R.)_{\gamma 2}}{\rho}\frac{\langle J(J-1)\rangle k^2}{\langle J\rangle^2(1-k)^2}\;\frac{b^2}{\omega^2+b^2}\right\}.$$

(171)

If we compare this result with that of equation (105) for the infinite model, we find that the frequency behavior of the power spectral densities corresponds very closely in each case. It is seen that a_1 in the infinite case is replaced by b in the finite case and that k_∞ goes over to

$$\frac{k_\infty}{1+L^2B_o^2}\quad, \text{ where}$$

$$L^2 \equiv \frac{D_1}{r_{aN}}\quad. \tag{172}$$

The only significant difference between equations (171) and (105) for the finite and infinite cases, respectively, can be shown to involve the count rates that multiply into the frequency dependent term of $\Phi(\omega)$ in each instance. If we denote the count rate in the finite model by $(C.R.)_{\gamma f}$ and in the infinite model by $(C.R.)_{\gamma\infty}$, it is easily shown that

$$\frac{(C.R.)_{\gamma f}}{(C.R.)_{\gamma\infty}} = \Omega_1(z,a)\quad.$$

(173)

Thus if $\Delta\Omega_1(z, a)$ becomes too small in a given one-detector experiment, it is clear that the frequency dependence of the power spectral density will not be observable in that experiment. In order to get a feeling for the distance that a photon detector may be placed from the core and the degree of photon collimation that is allowable such that $\Delta\Omega_1(z, a)$ remains at a reasonable value, let us consider the following example:

(1) a cubical reactor surrounded by a water moderator

(2) the detector is placed one photon mean free path from the core

(3) $a/z = .707$, i.e. $\arctan \frac{a}{z} = \frac{\pi}{4}$.

Performing the necessary computation, one finds for this example that $\Delta\Omega_1(z, a) = .007$. Applied to the example we considered previously for the infinite model, it is apparent that the photon detector in a real experimental situation will most likely have to be placed less than a mean free path, λ_{H_2O}, from the core and with very little collimation imposed on the photons impinging upon the detector. Of course considerable optimization of the many factors considered up to now must be carried out for each and any specific proposed experiment of this type.

Because of the difficulties with solid angle efficiencies, it is suggested from the theoretical expression for $\Phi(\omega)$ in equation (171) that a cross power spectral density (C. P. S. D.) experiment be

considered. In this case $A(D_1 \cap D_2) = 0$, and

$$\Phi(\omega) = \frac{\alpha (C.R.)_{\gamma 1} (C.R.)_{\gamma 2}}{2\rho} \frac{\langle J(J-1) \rangle k^2}{\langle J \rangle^2 (1-k)^2} \frac{b^2}{\omega^2 + b^2} \quad . \tag{174}$$

Thus in principle it appears that a C. P. S. D. experiment will yield information over a much broader range of power levels due to the extra factor, $(C.R.)_{\gamma 2}$, which now appears in the numerator along with the fact that the frequency dependent part of $\Phi(\omega)$ does not have to compete with the constant term, presumably due to white noise due to detector statistics, that previously appeared in $\Phi(\omega)$ for the one detector experiment. However, in practice an error analysis applied to the data handling process reveals that the C. P. S. D. experiment does not in fact enjoy the clear-cut superiority in all cases that is indicated by the above idealized theory.

b. The variance. (consider one detector experiment)

By integrating (139) twice from t = 0 to t, using the boundary conditions, zeroth modes, and the averaging procedure of the previous section, we find in the same manner as above

$$\frac{V}{M} - 1 = \frac{\alpha (C.R.)_{\gamma f}}{\rho} \frac{k^2 \langle J(J-1) \rangle}{\langle J \rangle^2 (1-k)^2} \left[1 - \frac{1 - e^{-bt}}{bt} \right] \quad . \tag{175}$$

This result is seen to correspond closely to (129) for the infinite model except that a_1 is replaced by b, and $\frac{V}{M} - 1$ is reduced by the factor $\Omega_1(\tau, a)$ as was the case for the frequency dependent part of the power spectrum as well. Thus once again it is virtually necessary to avoid very small solid angle efficiency factors $\Omega_1(\tau, a)$.

IV. APPLICATION TO AN ANALYSIS OF THE BROWN-TWISS CORRELATOR EXPERIMENT

A. Description of the System

We can note that the system of the Brown and Twiss correlator experiment appears to possess similar basic features as the systems we have investigated in previous chapters, and it should therefore be amenable to a transport theoretic interpretation. That is, the Brown-Twiss system is again one in which energy is transferred and in which modal and diffraction effects are absent. In this experiment a mercury arc source is filtered (4358 Å) and imaged on a pinhole .019 cm in diameter. The beam from this secondary source is then split by a half-silvered mirror, and the resultant beams are observed by photocathodes placed at equal optical distances from the source. One photocathode is stationary in the transmitted beam and the other photocathode is on a movable slide and can assume positions across the reflected beam. The outputs from the detectors are fed to a correlator which records the expectation value of the product of the fluctuations in the detector output currents.

That diffraction effects are expected to be negligible in this system is easily seen from the fact that all relevant dimensions of the system are much greater than the wavelength of the radiation. From a consideration of the radiation bandwidth used in this experiment it is found that the lifetimes of emitting states are short

compared to observation intervals. It can also be shown that coupling effects between the radiation field and the source atoms can be neglected. That is, the auto-covariance for source atoms and photon densities is effectively zero. One can further note that dimensions of the mercury arc source are small compared to the photon mean free paths in the source. Thus it is a good approximation to neglect photon absorption in the source, and it is also neglected in the interspace between the source and the detectors. The half-silvered mirror which splits the beam is considered to be a photon scatterer that deflects approximately half of the photons from the incident beam into what we have called the reflected beam. The photons from the beam incident to the mirror that are not scattered (reflected by the mirror) are transmitted and constitute what we have called the transmitted beam.

B. Specialization of the Transport Equations

In light of the above remarks and referring to Figure 4, we employ a model in which the photon source, $S(\underline{x},\underline{\Omega})$, is taken to be a disc (.019 cm diameter) from which photons are being emitted randomly by spontaneous emission. The photon and source atom distributions are assumed to be stationary. However when photons are detected by the photocathodes, the resultant photoelectrons are simply recorded (assume no loss mechanism for β's); and the number of photoelectrons recorded merely accumulates with time. The same boundary conditions obtain for charged particle densities

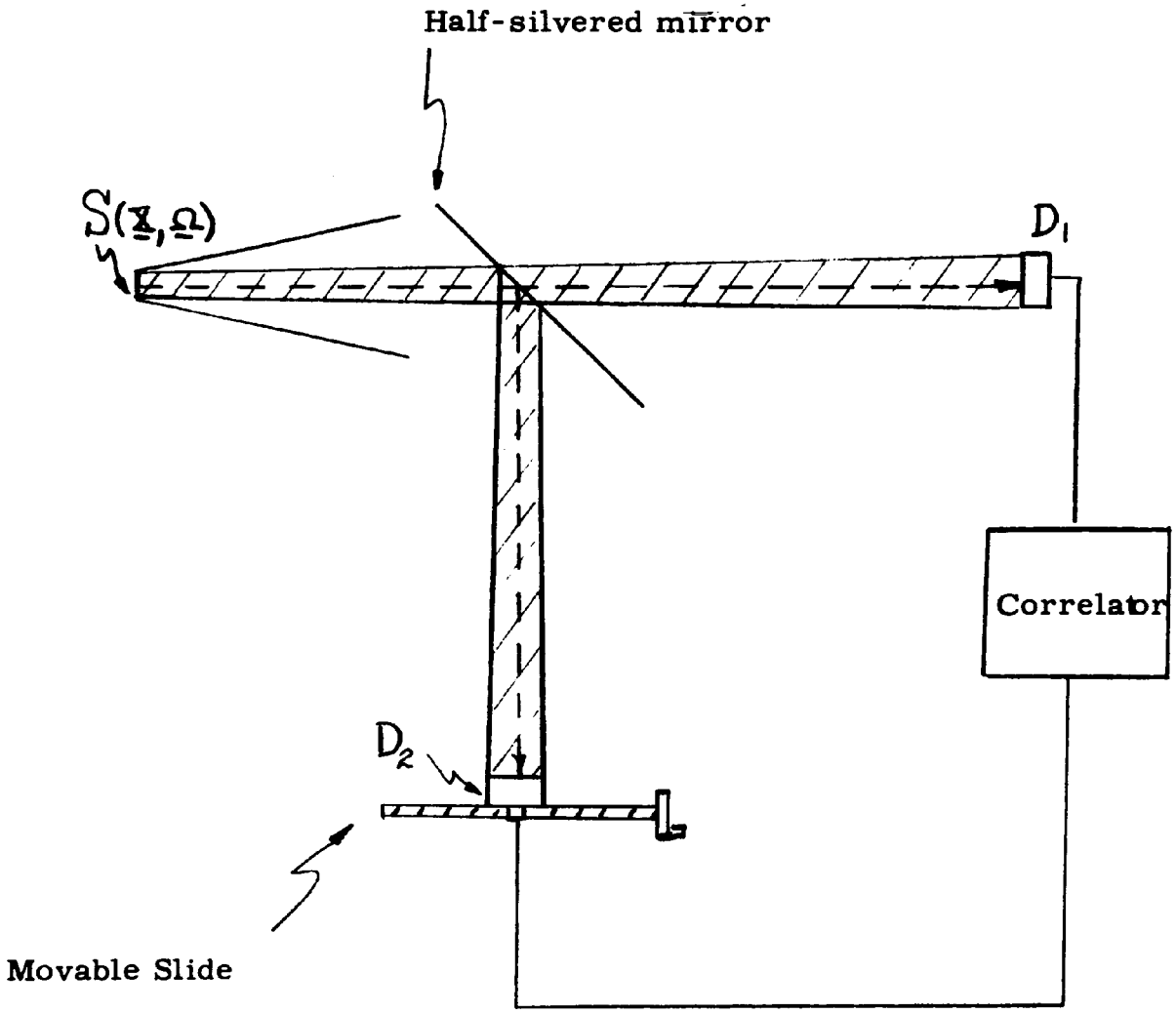


Figure 4. A Schematic Diagram of the System for the Brown and Twiss Correlator Experiment

here as in Chapter III. We then neglect streaming of photoelectrons and integrate their densities over their entire range of energies and directions. The densities necessary for the interpretation of this experiment are the singlets, doublets, and cross densities for photons and photoelectrons. Taking proper account of photon scattering in the deduction of the transport equations for this system, the reduced set of equations may then be obtained and written as:

$$\frac{\partial f_1^{\beta}(\underline{X},t)}{\partial t} = \Delta f_1^{\lambda}(\underline{X})\,H(t) \tag{176}$$

$$\frac{\partial f_2^{\beta\beta'}(\underline{X},\underline{X}',t)}{\partial t} = \left\{\Delta f_2^{\lambda\beta'}(\underline{X},\underline{X}',t) + \Delta' f_2^{\beta\lambda'}(\underline{X},\underline{X}',t)\right\}H(t) +$$

$$+ \delta(\underline{X}-\underline{X}')\,\Delta f_1^{\lambda}(\underline{X})\,H(t) \tag{177}$$

$$\left[c\,\underline{\Omega}\cdot\underline{\nabla} + r_{s\gamma}(\underline{X})\right] f_1^{\lambda}(\underline{X},\underline{\Omega}) = S(\underline{X},\underline{\Omega}) +$$

$$+ \int d\Omega''\, r_{s\gamma}(\underline{X})\, \mathcal{P}^{sc}(\underline{\Omega}''\rightarrow\underline{\Omega})\, f_1^{\lambda}(\underline{X},\underline{\Omega}'') \tag{178}$$

$$\left[c(\underline{\Omega}\cdot\underline{\nabla} + \underline{\Omega}'\cdot\underline{\nabla}') + r_{s\delta}(\underline{X}) + r_{s\delta}(\underline{X}')\right] f_2^{\lambda\lambda'}(\underline{X},\underline{\Omega};\underline{X}',\underline{\Omega}') =$$

$$= \int d\Omega''\, r_{s\delta}(\underline{X})\, \mathcal{J}^{sc}(\underline{\Omega}''\to\underline{\Omega})\, f_2^{\lambda\lambda'}(\underline{X},\underline{\Omega}'';\underline{X}',\underline{\Omega}') +$$

$$+ \int d\Omega''\, r_{sr}(\underline{X}')\, \mathcal{J}^{sc}(\underline{\Omega}''\to\underline{\Omega}')\, f_2^{\lambda\lambda'}(\underline{X},\underline{\Omega};\underline{X}',\underline{\Omega}'') +$$

$$+ S(\underline{X},\underline{\Omega})\, f_1^{\lambda'}(\underline{X}',\underline{\Omega}') + f_1^{\lambda}(\underline{X},\underline{\Omega})\, S(\underline{X}',\underline{\Omega}') +$$

$$+ \delta(\underline{X}-\underline{X}')\Big\{\delta(\underline{\Omega}-\underline{\Omega}')\Big[S(\underline{X},\underline{\Omega}) + r_{s\delta}(\underline{X})\, f_1^{\lambda}(\underline{X},\underline{\Omega}) +$$

$$+ \int d\Omega''\, r_{s\delta}(\underline{X})\, \mathcal{J}^{sc}(\underline{\Omega}''\to\underline{\Omega})\, f_1^{\lambda}(\underline{X},\underline{\Omega}'')\Big] - r_{s\delta}(\underline{X})\, \mathcal{J}^{sc}(\underline{\Omega}\to\underline{\Omega}')\, f_1^{\lambda}(\underline{X},\underline{\Omega}) -$$

$$- r_{sr}(\underline{X}')\, \mathcal{J}^{sc}(\underline{\Omega}'\to\underline{\Omega})\, f_1^{\lambda'}(\underline{X}',\underline{\Omega}')\Big\} \quad , \qquad (179$$

and

$$\left[\frac{\partial}{\partial t} + c\underline{\Omega}'\cdot\underline{\nabla}' + r_{s\gamma}(\underline{X}')\right] f_2^{\beta\lambda'}(\underline{X};\underline{X}',\underline{\Omega}';t) = \Delta f_2^{\lambda\lambda'}(\underline{X};\underline{X}',\underline{\Omega}')H(t) +$$

$$+ f_1^{\beta}(\underline{X},t)\,S(\underline{X}',\underline{\Omega}') + \int d\Omega''\, r_{s\gamma}(\underline{X}')\,\mathcal{J}^{sc}(\underline{\Omega}''\rightarrow\underline{\Omega}')\,f_2^{\beta\lambda'}(\underline{X},\underline{X}',\underline{\Omega}'',t) -$$

$$- \delta(\underline{X}-\underline{X}')\,r_D\,f_1^{\lambda}(\underline{X},\underline{\Omega}')H(t) \qquad (180)$$

The photon scattering frequency $\mathcal{J}^{sc}(\underline{\Omega}''\rightarrow\underline{\Omega})$ is defined analogously to that which was used previously for neutrons in equation (17), and $r_{s\gamma}(\underline{X})$ represents the photon scattering rate per photon. It is to be noted that $r_{s\gamma}(\underline{X})$ is a very localized function of position, in that it is zero everywhere except at the mirror. Also in these equations $C = 3 \times 10^{10}$ cm/sec is the speed of light as the media are assumed to be non-dispersive.

C. The Experimental Observables

It has been assumed up to now that the connection between the actual experiment and the theoretical interpretation is accomplished through the charged particle singlet and doublet density. That this is in fact the case can be seen as follows:

It is assumed that the correlator used by Brown and Twiss measured the expectation value of the product of the fluctuations in the output currents $\Delta\mathcal{J}_1(t)$ and $\Delta\mathcal{J}_2(t+\tau)$, where the subscripts designate the detectors. The observable, $\mathcal{O}$, is given by

$$\mathcal{O} = \frac{1+P}{2}\int_{\tau=0}^{T_R} d\tau \langle \Delta\mathcal{J}_1(t)\,\Delta\mathcal{J}_2(t+\tau)\rangle . \tag{181}$$

Using $\Delta\mathcal{J}(t) = \mathcal{J}(t) - \langle\mathcal{J}(t)\rangle$, this reduces to

$$\mathcal{O} = \frac{1+P}{2}\int_{\tau=0}^{T_R} d\tau \left\{\langle\mathcal{J}_1(t)\,\mathcal{J}_2(t+\tau)\rangle - \langle\mathcal{J}_1(t)\rangle\langle\mathcal{J}_2(t+\tau)\rangle\right\} . \tag{182}$$

The angular brackets stand for the expectation value which is obtained in practice by appropriate averaging procedures on the data from a large number of experimental runs. P is simply a permutation operator which interchanges 1 and 2. The integration over τ expresses the fact that the correlator performs the multiplication of $\mathcal{J}_1(t)$ and $\mathcal{J}_2(t+\tau)$ only for those detector currents arriving at the correlator within times τ between zero and T_R of each other. T_R is effectively the resolving time of the multiplying circuit in the correlator. Of course we recognize $\frac{1+P}{2}\langle\mathcal{J}_1(t)\,\mathcal{J}_2(t+\tau)\rangle$ as $\mathcal{G}(\tau)$, the generalized cross-correlation function, which is a function only of the lag time τ for stationary processes. For stationary currents we again use

$$\varphi(\tau) = \frac{1}{2} \frac{\partial^2 f_2^{\beta\beta'}(\tau)}{\partial \tau^2} \tag{183}$$

and

$$\frac{\partial f_1^{\beta_{1,2}}(t)}{\partial t} = \langle \vartheta_{1,2}(t) \rangle = \text{constant} . \tag{184}$$

Utilizing equations (183) and (184) in the expression for the observable given by (182), we find that the observable can be written as:

$$\mathcal{O} = \int_{\tau=0}^{T_R} d\tau \, \frac{1}{2} \frac{\partial^2 V^{\beta\beta}(\tau)}{\partial \tau^2} \tag{185}$$

where the variance, $V^{\beta\beta}(\tau)$ was defined previously. The photoelectron variance has been integrated over detector volumes $(D.V.)_1$ and $(D.V.)_2$ as shown in equation (186):

$$V^{\beta\beta}(\tau) \equiv \int_{(D.V.)_1} d^3\mathbf{x} \int_{(D.V.)_2} d^3\mathbf{x}' \, V^{\beta\beta}(\underline{x}, \underline{x}', \tau) . \tag{186}$$

D. A Qualitative Interpretation of the Results of Brown and Twiss

Brown and Twiss found that the measure of correlation observed by their correlator was maximized when the position of the movable detector, D_2 , in the reflected beam corresponded identically to the position of D_1 in the transmitted beam (as shown in Figure 4). As detector D_2 was moved to positions farther and farther out of correspondence with detector D_1 , the correlation continued to decrease more and more. Finally there was virtually no observable correlation when D_2 was out of those parts of the reflected beam that corresponded to the position of D_1 in the transmitted beam. That is to say there was relatively more (or less) correlation when D_2 could "see" relatively more (or less) of the same region of the beam incident upon the half-silvered mirror as was "seen" by D_1 .

Since the photons in the incident beam have a random distribution (having been born by spontaneous emission from a randomized assembly of source atoms) and since these photons are being detected by two physically distinct and separated detectors, one can ask, "Why, in fact, should there be any correlation at all?" Rather than solving the set of transport equations at this point (this is a straightforward, but sizable, task that will be presented in a subsequent paper), we can instead gain some insight into the physics of this problem by a qualitative consideration of the set of transport equations (176)-(180) and their associated boundary conditions. From the photon singlet

equation for this system, we can establish that subsequent to its birth a photon is only able to stream and to be either transmitted or reflected by the half-silvered mirror prior to detection. Recall that no photon absorption occurs in the interspaces. Thus a photon within the shaded area (see Figure 4) incident upon the half-silvered mirror must either be transmitted to detector D_1 or be scattered (reflected) to detector D_2 (provided D_2 is not in a region of the reflected beam that does not correspond to the same part of the beam seen by D_1). We therefore conclude that the correlation that is observed in this case must be due to the fact that the photon events at the mirror have altered the initially random distribution of the photons (represented by $\times$'s in Figure 5) in the incident beam.

This conclusion can perhaps be amplified with the help of Figure 5. We are considering now that portion of the incident beam represented by B_S that is "seen" by detector D_1 . For illustrative convenience consider the half-silvered mirror to be placed at an angle of 45° to the line of sight between the centers of the photon source and detector D_1 . Then assume that the mirror either transmits photons of the incident beam or scatters them through an angle of 90°. The photons scattered from B_S then define the reflected beam at 90° to the transmitted beam as shown in Figure 5. For the present we are considering D_2 to be positioned directly in the reflected beam (indicated in Figure 5 by position (a)) so that it "sees" B_S identically as D_1 "sees" it. We can now observe that the mirror

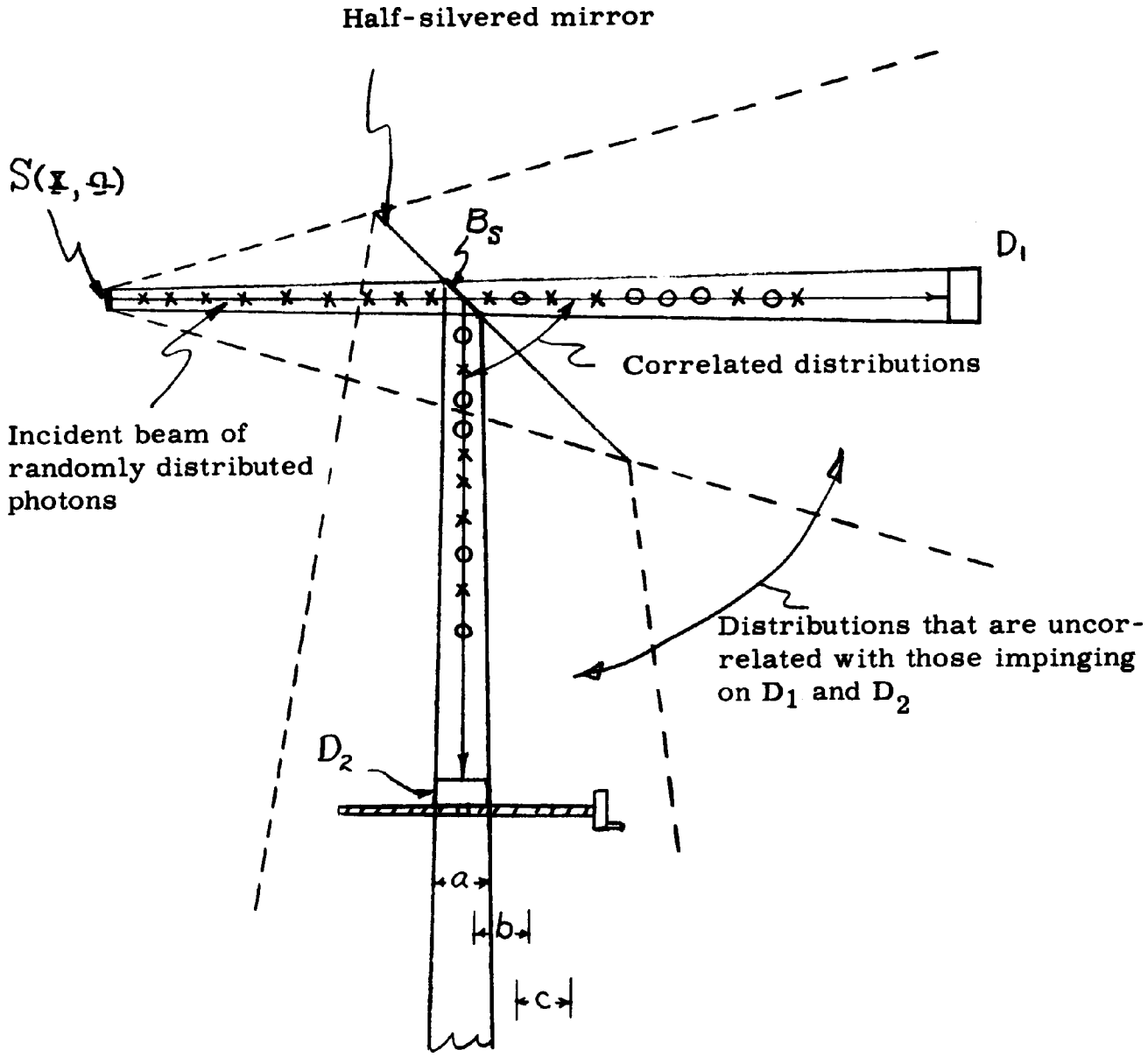


Figure 5. A Schematic Diagram to Exhibit the Role of the Half-Silvered Mirror in the Brown-Twiss Correlator Experiment

functions in such a manner that the transmission of an incident photon by the mirror, while introducing a photon into the transmitted beam, at the same time accounts for the absence (represented by o's in Figure 5) of a photon in the reflected beam. We might say that the mirror creates an "either-or" situation so far as the photons are concerned. That is, "either" they are transmitted and arrive eventually at detector D_1 "or" they are reflected and eventually arrive at detector D_2 . It is because of this situation created by the effect of the mirror that there is a one-to-one correspondence between the photons in one beam and the absence of photons in the other beam. We therefore conclude that this complete correspondence that has been introduced into the distribution of the photons in the transmitted and reflected beams accounts for the correlation that Brown and Twiss observed.

If we now consider the case when the detector D_2 is displaced to a position such as that shown by (c) in Figure 5, there is no correlation. This is because detector D_2 is unable to "see" that part of the beam, B_s , that corresponds to the region of the beam that is detected by D_1 . In other words the presence or absence of photons in the beam arriving at position (c) is totally independent of the presence or absence of photons in the beam striking detector D_1 . This can be referred to as the condition of no "correlation overlap." We have already considered the condition of complete "correlation overlap." This occurred when detector D_2 was in position (a) shown by

Figure 5. In this idealized case "correlation overlap" decreases linearly (is a function of the area of "overlap") as detector D_2 is moved from position (a) to intermediate positions (b), and is of course zero in position (c).

Our discussion up to now has been for an idealized situation in which we have assumed for instance that the detection efficiencies of D_1 and D_2 are constant and uniform over the detector faces as well as that the beam intensity of correlated photons is uniform for all detector positions. Of course these conditions are not fulfilled in practice. An additional factor is that in practice the half-silvered mirror tends to spread the reflected beam so that the region of the reflected beam containing "correlated" photons is broader than the beam seen by detector D_1. In Figure 6 we plot the data points of Brown and Twiss as well as what we shall call the ideal correlation factor (dotted line) that represents our theoretical observable, $\mathcal{O}$. This is seen to fall below their data points in Figure 6 and goes to zero at d = 5mm (this is the size of the detector apertures used in the Brown and Twiss experiment). Therefore when the region containing "correlated" photons is broadened, as we have mentioned above, and when we account for the fact that the intensity of "correlated" photons is significantly reduced in the broadened regions of the reflected beam (as compared to that intensity in the central region) we expect suitable agreement between our theoretical interpretation and the experimental results of Brown and Twiss. The abscissa of Figure 6

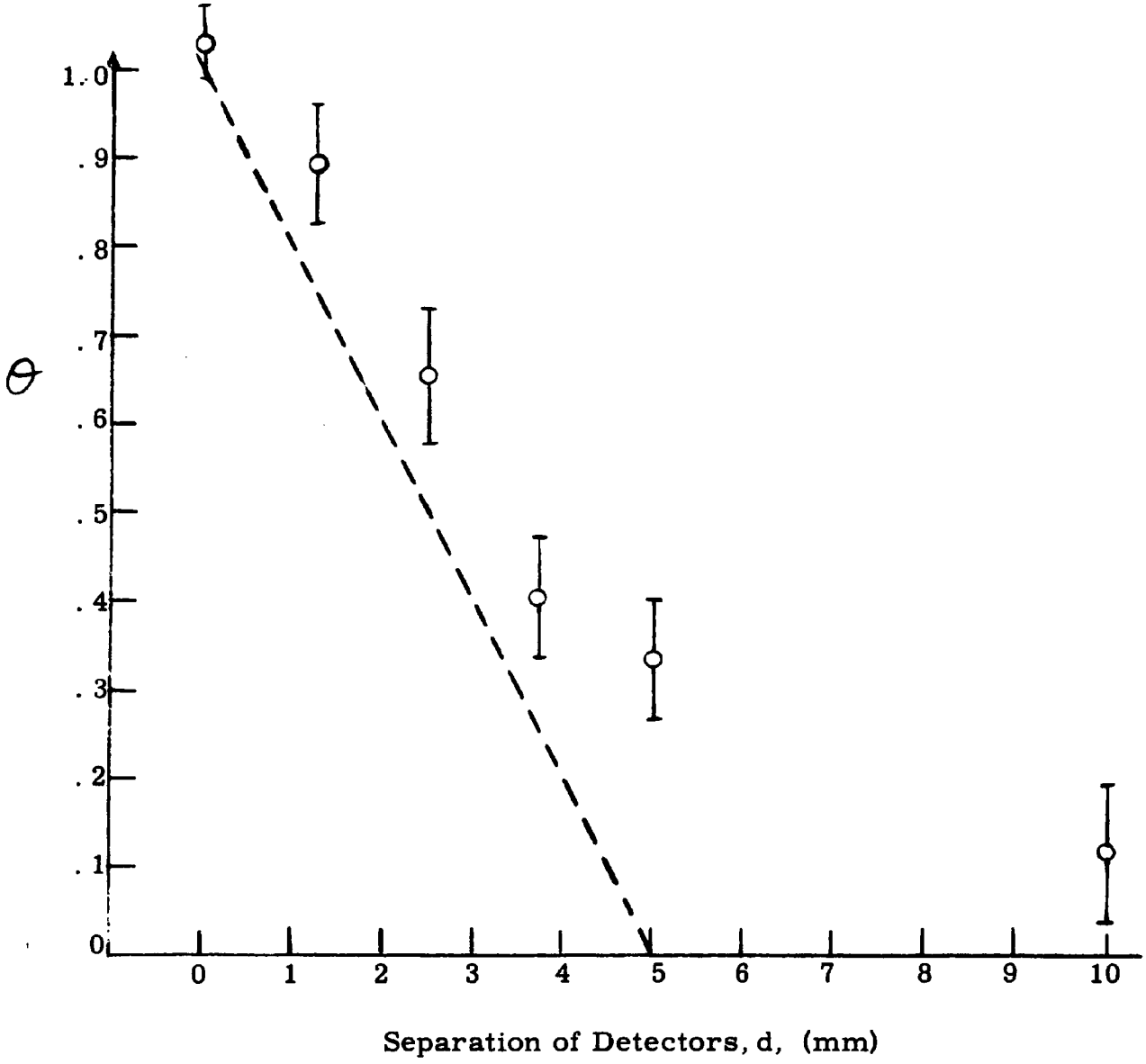


Figure 6. Ideal Correlation Factor versus Detector Separation in Brown-Twiss Correlator Experiment

is referred to as the separation of the detectors, d. This is effectively the separation of the centers of D_1 and D_2 relative to each other using the centers of the transmitted and reflected beams as a reference point.

There is the implication from our interpretation that the effect observed by Brown and Twiss is largely dependent upon geometric considerations and is most likely insensitive to stimulated emission (sometimes referred to as "photon bunching" effects due to quantum statistics) and to coupling effects (or lack of them) between the radiation field and the source atoms. It is furthermore interesting to note that Brown and Twiss[21] made the observation very early that their results indicated this dependence upon the geometry of the system.

Finally instead of using a correlator to determine the measure of correlation, we can suggest an experiment which measures the ratio of the cross-covariance of the photoelectron counts from D_1 and D_2 to the mean of the counts obtained from D_1. This experiment would seem to be more directly interpretable. That is, with the appropriate data handling equipment the pulses generated by the detection events can be recorded directly onto a video tape, provided the count rates do not get too high. This information can then be processed to yield the quantities $f_2^{\beta\beta}(\tau)$, $f_1^{\beta_1}(\tau)$, and $f_1^{\beta_2}(\tau)$ directly as a function of gate width τ of the data processing operation and from the displacement of detector D_2. There would be no uncertainty then

as to the connection between the experimental observables and the theory, because the accumulants $f_2^{\beta_1\beta_2}(\tau)$, $f_1^{\beta_1}(\tau)$, and $f_1^{\beta_2}(\tau)$ of photoelectrons in an interval τ are directly available both experimentally and theoretically.

V. GENERAL PROPERTIES OF RADIATION DISTRIBUTIONS

In this chapter we will briefly examine in finer detail some of the rather interesting properties of exclusively the radiation distributions. It was indicated in Chapter IV that the Brown-Twiss correlator experiment using a spontaneously emitting, random photon source most likely gives no information about the dynamics of the source system since it is largely a geometric effect. From here on we will refer to random photon sources such as their mercury arc as "Poisson-like" inasmuch as it can be shown that the variance of the radiation distribution is equal to the mean. It is therefore implied that non-"Poisson-like" radiation distributions in some ways may be of more interest, so far as obtaining information about dynamic parameters of a system is concerned, in the type of correlation experiments that we consider. A case that illustrates this point occurred in the reactor noise applications where we saw that dynamic parameters of the interacting system (the nuclear reactor) were obtainable, in principle, from radiation with a non-"Poisson-like" distribution, as compared to the fundamentally simpler correlation effect observed in the Brown-Twiss experiment. In the reactor noise application the multiple production of photons and of neutrons from neutron interactions accounted for the departure of the radiation distribution from Poisson. We then might ask, "What type of correlation properties might we observe in a fluctuation experiment if we use a

different optical source, say, a black body radiating source, where stimulated emission may account for a departure of the radiation distribution from Poisson; and what other relevant measurements might thereby be suggested on such a system?" The sections that follow in this chapter deal with these matters and will examine some of the ramifications that arise from considering the characteristics of "Poisson-like" and non-"Poisson-like" optical sources.

A. Specialization of the Equations for Photon Singlet and Doublet Densities

In light of our above remarks let us consider a spatially dependent model of an infinite homogeneous medium in which photon scattering is neglected and photon occupation numbers are retained (as compared to unity). This in effect accounts for stimulated emission. We use the conventional notation of $\alpha(\underline{k})$ to represent the absorption rate of photons with wave vector $\underline{k}$ and $\epsilon(\underline{k})$ to represent the emission rate of photons with wave vector $\underline{k}$. Then assuming that the photon densities are stationary, the reduced equations are obtained in the same way as previously. Thus the photon singlet equation is given as

$$\left[c\,\underline{\Omega}\cdot\underline{\nabla} + \alpha(\underline{k}) - \epsilon(\underline{k})\right] f_1(\underline{r},\underline{k}) = \epsilon(\underline{k})\rho_{\underline{k}} \qquad (187)$$

where the medium is again taken to be non-dispersive; and the photon doublet equation is given as

$$\left[c(\underline{\Omega}\cdot\underline{\nabla} + \underline{\Omega}'\cdot\underline{\nabla}') + (\alpha(\underline{k}) - \epsilon(\underline{k})) + (\alpha(\underline{k}') - \epsilon(\underline{k}'))\right] f_2^{\lambda\lambda'}(\underline{x},\underline{k};\underline{x}',\underline{k}') =$$

$$= \epsilon(\underline{k})\rho_k f_1^{\lambda'}(\underline{x}',\underline{k}') + f_1^{\lambda}(\underline{x},\underline{k})\epsilon(\underline{k}')\rho_{k'} + \delta(\underline{x}-\underline{x}')\,(*)$$

$$(*)\,\delta(\underline{k}-\underline{k}')\left\{\left[\alpha(\underline{k}) + \epsilon(\underline{k})\right] f_1^{\lambda}(\underline{x},\underline{k}) + \epsilon(\underline{k})\rho_k\right\}.$$

(188)

If we introduce

$$a(\underline{k}) \equiv \alpha(\underline{k}) - \epsilon(\underline{k}) \tag{189a}$$

and

$$a(\underline{k}') \equiv \alpha(\underline{k}') - \epsilon(\underline{k}') \tag{189b}$$

and

$$H(\underline{x},\underline{k}) \equiv \left[\alpha(\underline{k}) + \epsilon(\underline{k})\right] f_1^{\lambda}(\underline{x},\underline{k}) + \epsilon(\underline{k})\rho_k \quad , \tag{190}$$

we can write the equation for the photon variance as

$$\left[c(\underline{\Omega}\cdot\underline{\nabla} + \underline{\Omega}'\cdot\underline{\nabla}') + a(\underline{k}) + a(\underline{k}')\right] V^{\lambda\lambda'}(\underline{x},\underline{k};\underline{x}',\underline{k}') =$$

$$= \delta(\underline{x}-\underline{x}')\,\delta(\underline{k}-\underline{k}')\,H(\underline{x},\underline{k}) .$$

(191)

In the model we are using, the medium is infinite in the sense that the photon singlet density is spatially independent. However the photon doublet density is spatially dependent.

B. Solutions of the Equations and Discussion

The solution of (191) is straightforward by Fourier transformation with respect to both $\underline{X}$ and $\underline{X}'$ (as done previously), and the result is

$$V^{\lambda\lambda'}(\underline{X},\underline{k};\underline{X}',\underline{k}') = \frac{\delta(\underline{X}-\underline{X}')\delta(\underline{k}-\underline{k}')H(\underline{k})}{2[\alpha(\underline{k})-\epsilon(\underline{k})]} \tag{192}$$

or

$$V^{\lambda\lambda'}(\underline{X},\underline{k};\underline{X}',\underline{k}') = \frac{\delta(\underline{X}-\underline{X}')\delta(\underline{k}-\underline{k}')}{2[\alpha(\underline{k})-\epsilon(\underline{k})]}\left\{[\alpha(\underline{k})+\epsilon(\underline{k})]f_1^{\lambda}(\underline{k})+\epsilon(\underline{k})\rho_{\underline{k}}\right\}. \tag{193}$$

If we are looking at a black-body system in which the atoms are in equilibrium at a temperature T, it can be shown that

$$\alpha(\underline{k}) = \epsilon(\underline{k})\exp \varepsilon_k/\theta \tag{194}$$

We have introduced

$$\mathcal{E}_{\underline{k}} \equiv \hbar c \underline{k} \tag{195}$$

and

$$\theta = kT \tag{196}$$

where k is Boltzmann's constant. Therefore the equilibrium distribution for the photon singlet density is

$$f_1^{\lambda}(\underline{k}) = \frac{\rho_{\underline{k}}}{e^{\mathcal{E}_{\underline{k}}/\theta} - 1} \tag{197}$$

Recall that $f_1^{\lambda}(\underline{k})$ is defined to be a density per unit $\underline{K}$-volume. This of course goes over to the more conventional form for black-body radiation, by defining, as Klevans[13] did, an energy density $U(\underline{k}) \equiv \hbar c \underline{k} f_1^{\lambda}(\underline{k})$. Then using $\rho_{\underline{k}} = 1/(2\pi)^3$, transforming to frequency space, using $2\pi \nu_{\lambda} = c \underline{k}$, and summing over polarizations, λ, we get

$$U(\nu) = \frac{8\pi h}{c^3} \frac{\nu^3}{e^{h\nu/\theta} - 1} \tag{198}$$

The expression for the ratio of the photon variance to the mean becomes

$$\frac{V^{\lambda\lambda'}(\underline{X}, \underline{k}; \underline{X}', \underline{k}')}{f_1^{\lambda}(\underline{k})} = \frac{\delta(\underline{X} - \underline{X}')\,\delta(\underline{k} - \underline{k}')}{1 - e^{-\mathcal{E}_{\underline{k}}/\theta}} \tag{199}$$

Recall that we are actually working with discrete points in phase space, and let $\underline{x}' = \underline{x}$. Then integrating over $\underline{X}'$ and averaging equation (199) over $\underline{X}$, considering the system to be large enough that our prior assumptions for this model hold, we find

$$\frac{V^{\lambda\lambda}(\underline{x})}{f_1^{\lambda}(\underline{x})} = \frac{1}{1 - e^{-\varepsilon_x/\theta}} \tag{200}$$

This result is in agreement with that of Landau and Lifshitz[23]. Of course the chemical potential, denoted by μ , in their result for Bose-Einstein particles becomes zero when considering radiation.

We now recognize from (198) or (199) that if $\varepsilon_x >> \theta$ the radiation distribution is "Poisson-like" even in the presence of stimulated emission. Recall that in the experiment performed by Brown and Twiss there was virtually no stimulated emission in the source. It appears now that, even if there were an appreciable amount of stimulated emission in the source, a measurement on the high energy tail of the radiation distribution would not be able to distinguish the effects of stimulated emission that are present. By implication the measurement of dynamic parameters of the system would not be feasible by this type of observation. On the other hand it is expected that the fluctuations could be exceedingly large and the stimulated emission effects quite pronounced in an observation if this measurement were performed on the very low energy $(\varepsilon_x << \theta)$

radiation. To perform a more realistic calculation in a given instance to get some quantitative estimate for the magnitude of the fluctuations that might be expected in an actual experimental situation, equation (193) can be solved for $V^{\wedge}(\underline{x},\underline{\kappa};\underline{x}',\underline{\kappa}')$ in a manner analogous to our previous work on the finite reactor and finite detector system that appeared in Chapter III.

Finally we can discuss the results we have obtained by a transport theoretic approach and make a few observations regarding the "coherence properties" of our photon distributions in the context of Glauber's[8][24] "correlation functions." These "correlation functions," or Green's functions, are expectation values of normally-ordered products of creation and annihilation operators. The first and second order correlation functions at points $\underline{x}$ and $\underline{x}'$ at one time, t, and for photons with energy $\hbar c \kappa$ are defined by Glauber as:

$$G^{(1,1)}(\underline{x},\underline{x};t) \equiv Tr\ \alpha^{\dagger}(\underline{x})\,\alpha(\underline{x})\,D(t) \tag{201}$$

and

$$G^{(2,2)}(\underline{x},\underline{x};\underline{x}',\underline{x};t) \equiv Tr\,\alpha^{\dagger}(\underline{x})\,\alpha^{\dagger}(\underline{x}')\,\alpha(\underline{x}')\,\alpha(\underline{x})\,D(t). \tag{202}$$

Glauber points out that the first order correlation function $G^{(1,1)}(\underline{x},\underline{x}';t)$ (for $\underline{x} \neq \underline{x}'$) does not correspond to an ordinary

measurement, and this is a motivating factor for the correlation functions that he defines.

Now applying the commutation relationships

$$\left[\alpha(\underline{x}),\ \alpha^{\dagger}(\underline{x}')\right] = \delta(\underline{x} - \underline{x}') \tag{203}$$

and

$$\left[\alpha(\underline{x}),\ \alpha(\underline{x})\right] = \left[\alpha^{\dagger}(\underline{x}),\ \alpha^{\dagger}(\underline{x})\right] = 0 \tag{204}$$

and assuming the photons to be in a stationary state, it is seen that

$$G^{(1,1)}(\underline{x},\underline{x}) = f_1^{\lambda}(\underline{x}) \tag{205}$$

$$G^{(1,1)}(\underline{x}',\underline{x}') = f_1^{\lambda'}(\underline{x}') \tag{206}$$

and

$$G^{(2,2)}(\underline{x},\underline{x}';\underline{x}',\underline{x}) = f_2^{\lambda\lambda'}(\underline{x},\underline{x}') - \delta(\underline{x} - \underline{x}')f_1^{\lambda}(\underline{x}). \tag{207}$$

Then considering Glauber's condition for second order coherence, which is defined as

$$G^{(2,2)}(\underline{X}, \underline{X}'; \underline{X}', \underline{X}) = G^{(1,1)}(\underline{X}, \underline{X}) \, G^{(1,1)}(\underline{X}', \underline{X}') \tag{208}$$

we see that for the present case this condition can be stated as

$$V^{\lambda\lambda'}(\underline{X}, \underline{X}') = \delta(\underline{X} - \underline{X}') \, f_1^{\lambda}(\underline{X}) \, . \tag{209}$$

Therefore Glauber's condition of second order coherence is satisfied by "Poisson-like" sources. Of course a spontaneously emitting photon source with no photon absorption and no coupling between the photon field and the emitting atoms is such a source. We have also seen that a system that is observed by the detection of photons with energies $\mathcal{E}_k >> \Theta$, even in the presence of stimulated emission, is also expected to satisfy Glauber's second order coherence condition. The analysis we have brought to bear earlier on the observables of the Brown-Twiss correlator experiment indicates that their experiment is dominated in the main by geometric considerations for systems satisfying the second order coherence condition, and are not expected to yield significant information regarding dynamic parameters of the interacting source system.

REFERENCES

1. Chang-Hwa Shen, "Noise Analysis of Pennsylvania State University Reactor," Pennsylvania State University, Master's Thesis (1964).

2. F. C. Maienshein, R. W. Peelle, W. Zobel, and T. A. Love, "Gamma Rays Associated with Fission," Second United Nations International Conference on the Peaceful Uses of Atomic Energy, A/Conf. 15/P/670, June, 1958.

3. G. T. Chapman, K. M. Henry, and J. D. Jarrard, "Pulse Height Spectra of Gamma Rays Emitted by the Stainless Steel Clad Bulk Shielding Reactor II (BSR - KK)," ORNL 3609, November, 1964.

4. R. Hanbury Brown and R. Q. Twiss, Proc. Roy. Soc. 243A, (1958).

5. W. Matthes, "Statistical Fluctuations and Their Correlation in Reactor Neutron Distributions," Nukleonik, Band 4, Heft 5, 213 (1962).

6. P. R. Pluta, "An Analysis of Fluctuations in a Boiling Water Reactor by Methods of Stochastic Processes," APED 4071, October 10, 1962.

7. D. R. Harris, "Stochastic Fluctuations in a Power Reactor," WAPD-TM-190, November, 1958.

8. R. J. Glauber, "Optical Coherence and Photon Statistics," Quantum Optics and Electronics, Edited by DeWitt, Blanden and Cohen-Tannoudji, Gordon and Breach, New York (1965).

9. R. K. Osborn and S. Yip, Proc. of the Noise Conference at the University of Florida, Trans. of ANS (1963), to be published as AEC monograph.

10. R. K. Osborn and M. Natelson, "Kinetic Equations for Neutron Distributions," Journal of Nuclear Energy, Part A/B, 19, 619 (1965).

11. S. Ono, Prog. Theor. Phys. (Japan) 12, 113 (1954).

12. R. K. Osborn, "Kinetic Equations for Fully Ionized, Inhomogeneous Plasmas," Phys. Rev., 130, 6, 2142 (1963).

13. E. H. Klevans, "A Theory of Photon Transport in Dispersive Media," UMRL Technical Report No. 2764-12-T (1962).

14. Z. Akcasu, to be published in Nuclear Science and Engineering (1966).

15. A. Papoulis, Probability, Random Variables, and Stochastic Processes, McGraw-Hill, New York (1965).

16. R. K. Osborn, "Speculations on the Interpretation of Neutron Noise Experiments," ORNL-3757, January, 1965.

17. R. W. Albrecht, "The Measurement of Dynamic Nuclear Reactor Parameters by Methods of Stochastic Processes," University of Michigan, PhD Thesis (1961).

18. C. W. Ricker, S. H. Hanauer, and E. R. Mann, "Measurement of Reactor Fluctuation Spectra and Subcritical Reactivity," ORNL-TM-1066, April, 1965.

19. M. Natelson, R. K. Osborn, and F. Shure, "Space and Energy Effects in Reactor Fluctuation Experiments," to be published in Journal of Nuclear Energy.

20. Theodore Rockwell III, Reactor Shielding Design Manual, United States Government Printing Office.

21. Herbert Goldstein, The Attenuation of Gamma Rays and Neutrons in Reactor Shields, United States Government Printing Office (1957).

22. R. Hanbury Brown and R. Q. Twiss, "Correlation between Photons in Two Coherent Beams of Light," Nature, 177, 27 (1956).

23. L. D. Landau and E. M. Lifshitz, Statistical Physics, Addison-Wesley, Reading, Mass. (1958).

24. R. J. Glauber, "Coherent and Incoherent States of the Radiation Field," Physical Review, 131, 6 (September 15, 1963).